Title
A STUDY OF THE REACTION K~Nu> SK FROM THRESHOLD TO 2.7 GeV/c.

Author
Muller, Richard A.

Publication Date
1969-08-08

UCRL-19372

cy. 2

A STUDY OF THE REACTION $K^-N \rightarrow \Xi K$ FROM THRESHOLD TO 2.7 GeV/c

Richard A. Muller
(Ph. D. Thesis)

August 8, 1969

AEC Contract No. W-7405-eng-48

LAWRENCE RADIATION LABORATORY
UNIVERSITY of CALIFORNIA BERKELEY

UCRL-19372

cy. 2

DISCLAIMER

The endless cycle of idea and action,

Endless invention, endless experiment,

Brings knowledge of motion, but not of stillness.

-- T. S. Eliot

A Study of the Reaction $K^-N \to \Xi K$ from Threshold to 2.7 GeV/c

Richard A. Muller

University of California
Berkeley, California

August 8, 1969

ABSTRACT

We have performed a partial wave analysis of the reactions $K^-p \to \Xi^-K^+$, $K^-p \to \Xi^0K^0$, and $K^-n \to \Xi^-K^0$. We used about 3000 events with beam momenta ranging from 1.2 to 2.7 GeV/c, obtained in the Berkeley 72 in. bubble chamber. We present new data for the reaction $K^-n \to \Xi^-K^0$ at 2.1 and 2.64 GeV/c. The total cross sections at these momenta are 69^{+14}_{-7} μb and 36^{+10}_{-5} μb respectively. The polarization was measured from the sequential weak decays $\Xi \to \Lambda\pi$, $\Lambda \to p\pi^-$. By assuming that the parts of the invariant amplitudes that are due to baryon exchange factorize into functions that depend only on s = (total center of mass energy)^2 and u = (4-momentum of exchanged baryon)^2, we generate powerful constraints on the partial wave amplitudes. Using these constraints we have done an energy dependent fit to the data. We conclude from the fit that the data can be explained in terms of isotopic spin 0 baryon exchange, with small but important contributions from isotopic spin 1 baryon exchange and direct channel resonance production. Only known Y^* resonances were included in the direct channel. The baryon exchange partial waves move in counter-clockwise circles in the Argand diagram, suggesting that they may have a "dual" interpretation as resonant partial waves.

I. INTRODUCTION

This study is an attempt to understand the reaction $K^-N \to \Xi K$ in terms of baryon exchange and direct channel resonance production. In particular we would like to answer the following questions:

Are the known resonances, i.e. Y^* resonances that have been studied in the elastic channel and in the total cross-section data, sufficient to explain all the data when combined with a reasonable parameterization for the "background"? If not, is there sufficient evidence to indicate the existence of one or more new resonances?

Can we understand the "background" in terms of particle (baryon) exchange? If so, can we learn anything about baryon exchange amplitudes from a study of our background?

In our analysis we used about 3000 events with beam momenta ranging from 1.2 to 2.7 GeV/c, obtained in the Berkeley 72" bubble chamber.[1-4] At three momenta -- 1.5, 2.1, and 2.6 GeV/c -- we have data for all three of the following reactions:

(1) $K^-p \to \Xi^-K^+$

(2) $K^-p \to \Xi^\circ K^\circ$

(3) $K^-d \to \Xi^-K^\circ$ + spectator proton

The approach we decided upon was an energy dependent partial wave analysis. In a partial wave analysis one expresses the total amplitude for the reaction in terms of "partial waves" which are complex functions of energy corresponding to definite spins and parities. This is the natural approach for studying direct channel resonances since a resonance has definite spin and parity and, therefore, contributes to only one

partial wave. Furthermore, the energy dependence of a resonance is adequately represented by a simple Breit-Wigner function with only two or three parameters.

Partial wave analysis is not, however, the usual way to study particle exchange amplitudes, which can contribute to many partial waves. Unfortunately (for the experimenter) there is no canonical way to study particle exchange amplitudes. One way is to take a detailed theoretical model, such as a Born term with absorption or a Regge exchange model, and attempt to fit it to the data.[5-7] What we tried to do instead was to develop a parameterization for the exchange amplitude which is consistent with a simple physical picture of particle exchange. Our parameters are the set of partial waves at some reference energy, and therefore partial wave analysis is as appropriate for the particle exchange terms as it is for the resonant terms.

The Ξ K reaction has several interesting and unusual features:

(a) We get a good measurement of the polarization of the Ξ from its cascade decay: $\Xi \to \Lambda\pi$, $\Lambda \to p\pi^-$.

(b) Meson exchange, which dominates many other reactions, is "forbidden" in ours because it would involve a strangeness 2 meson, and no such meson is known.[8]

(c) The existence of a strong "backward peak" in the differential cross sections at all energies above 1.2 GeV/c indicates that baryon exchange is important. There are both experimental and theoretical reasons to believe that the baryon exchange amplitude is confined to the lower partial waves ($J \lesssim \frac{3}{2}$).

(d) The known resonances in our energy region are confined to the higher partial waves, and are therefore distinct from the baryon exchange partial waves. This separation is important in view of recent theoretical work on the "duality" principle. (We discuss this point in greater detail in section IV.)

(e) The existence of data for all three of the above reactions enables us to determine the isotopic spin decomposition of the reaction amplitudes. By making the decomposition in the u-channel we can determine the isotopic spin of the exchanged baryons.

The remainder of this paper is organized as follows:

Section II. A summary of the formalism of partial wave analysis and isotopic spin decomposition as applied to our reactions.

Section III. Preliminary analysis of the deuterium data at 2.1 and 2.64 GeV/c. (The reduction of the rest of the data has been described elsewhere.)[1-4]

Section IV. Qualitative features of the data.

Section V. Model of baryon exchange and resonant partial waves. Description of the fitting program. Results of the fit.

Section VI. Conclusions.

II. FORMALISM

In this section we present the results of applying the conservation of parity, angular momentum, and isotopic spin to meson-nucleon scattering. The conventions used are:

q_1, m_1, e_1	momentum, mass, and energy of incoming meson
q_2, m_2, e_2	momentum, mass, and energy of outgoing meson
p_1, M_1, E_1	momentum, mass, and energy of incoming baryon
p_2, M_2, E_2	momentum, mass, and energy of outgoing baryon
W	total center of mass energy
$\cos(\theta)$	$\hat{q}_1 \cdot \hat{q}_2$ in center of mass
$\bar{M}$	$(M_1 + M_2)/2$
$\overline{E \pm M}$	$[(E_1 \pm M_1) \cdot (E_2 \pm M_2)]^{1/2}$

A. Parity

The amplitude for scattering from a state χ_i to a new state χ_f can be expressed as χ_f M χ_i where M is a 2 x 2 matrix. Parity conservation implies that M can be expanded in terms of two scalar (but not Lorentz invariant) functions as follows:

$$M = f + ig\vec{\sigma} \cdot \hat{n}$$

where $\vec{n} = \hat{q}_1 \times \hat{q}_2$ is the normal to the production plane and $\vec{\sigma}$ is the set of Pauli matrices. If the target baryon is unpolarized, then the differential cross section and final state polarization are given by

$$\frac{d\sigma}{d\Omega} = \frac{1}{2} \text{Tr } M^\dagger M = |f|^2 + |g|^2$$

$$\vec{P} \frac{d\sigma}{d\Omega} = \frac{1}{2} \text{Tr } M^\dagger \vec{\sigma} M = 2 \text{ Im } (fg^*)\hat{n}$$

M is sometimes defined in terms of amplitudes f_1 and f_2 where

$$M = f_1 + f_2 \vec{\sigma} \cdot \hat{q}_1 \vec{\sigma} \cdot \hat{q}_2$$

f_1 and f_2 are related to f and g as follows:

$$f = f_1 + f_2 \cos\theta$$

$$g = f_2 \sin\theta$$

If we express the transition amplitude in covariant form

$$-\bar{u}(p_2) \left[A + \frac{1}{2}(q_1 + q_2)_\mu \gamma_\mu B\right] u(p_1)$$

we explicitly display the two Lorentz invariant amplitudes A and B. These are related to the amplitudes f_1 and f_2 as follows:[5]

$$f_1 = \frac{1}{8\pi W}[(E_1 + M_1)(E_2 + M_2)]^{1/2}[A + (W-\bar{M})B]$$

$$f_2 = \frac{1}{8\pi W}[(E_1 - M_1)(E_2 - M_2)]^{1/2}[-A + (W + \bar{M})B]$$

B. Angular Momentum

The amplitudes f and g can be expressed as a sum of amplitudes of definite spin and parity as follows:

$$f = \frac{1}{p_1} \sum_\ell [(\ell + 1) T_\ell^+(W) + \ell T_\ell^-(W)] P_\ell(\cos\theta)$$

$$g = \frac{1}{p_1} \sum_\ell [T_\ell^+(W) - T_\ell^-(W)] P'_\ell(\cos\theta)$$

where

$$P^1_\ell(\cos\theta) = \sin\theta P'_\ell(\cos\theta) = \sin\theta \frac{dP_\ell(\cos\theta)}{d\cos\theta}$$

$T_\ell^\pm$ is the "partial wave" with orbital angular momentum ℓ and total angular momentum $J = \ell \pm 1/2$. Using the relationships that exist between the conventional amplitudes f and g, and the invariant amplitudes A and B, we write A and B in terms of the partial waves:

$$A = \sum (W^+ P'_{\ell+1} + W^- P'_\ell)\ T_\ell^+ + (-W^+ P'_{\ell-1} - W^- P'_\ell) T_\ell^-$$

$$B = \sum (E^+ P'_{\ell+1} - E^- P'_\ell)\ T_\ell^+ + (-E^+ P'_{\ell-1} + E^- P'_\ell) T_\ell^-$$

where $E^\pm$ and $W^\pm$ are the following kinematic functions:

$$E^\pm = \frac{4\pi}{p_1} \frac{1}{E \pm M}$$

$$W^\pm = (W \pm \bar{M}) \cdot E^\pm$$

We also refer to the partial waves using the optical notation $L_{2I,2J}$ or simply L_{2J} where L is S, P, D, F, . . . etc. for ℓ = 0, 1, 2, 3, . . ., I is the total s-channel isospin, and J is the total angular momentum.

C. Legendre Expansion Coefficients

The differential cross sections and polarizations for our three reactions can be expressed in terms of Legendre polynomials as follows:

$$\frac{d\sigma}{d\Omega} = \frac{\sigma}{4\pi} \sum_{\ell=0} \left(\frac{A\ell}{Ao}\right) P_\ell\ (\cos\theta)$$

$$P_\Xi \frac{d\sigma}{d\Omega} = \frac{\sigma}{4\pi} \sum_{\ell=1} \left(\frac{B\ell}{Ao}\right) P_\ell^1(\cos\theta)$$

where $Ao = \sigma/4\pi\lambda\!\!\!^{-2}$, and $\lambda\!\!\!^{-}$ is $\hbar$ divided by p_1, the initial state center of mass momentum. These expansions were carried out at our thirteen energies, using the method of moments[3] to obtain the coefficients A_L/A_0 and B_L/A_0; the results are shown in Figures 9-16 and Tables 2-5. The A_L's and B_L's can be expressed in terms of a sum of products of partial wave amplitudes as follows:[9]

$$A_\ell = \sum_{i<j} \alpha_\ell^{ij}\ \mathrm{Re}\ (T_i^* T_j)$$

$$B_\ell = \sum_{i<j} \beta_\ell^{ij} \text{ Im } (T_i^* T_j)$$

The coefficients α and β are given in Tables 1a and 1b.[10] The data can be qualitatively understood by looking at the energy dependence of the A_ℓ's and B_ℓ's, and using these tables to deduce which partial waves must be important. (See Section IV below.)

D. Isotopic Spin

The partial wave amplitudes for our three reactions can be decomposed into amplitudes having simple properties in either the direct, or a crossed channel. Using the conventions for the isospinors,[11]

$$\begin{pmatrix} p \\ n \end{pmatrix} \qquad \begin{pmatrix} \Xi^\circ \\ \Xi^- \end{pmatrix} \qquad \begin{pmatrix} K^+ \\ K^\circ \end{pmatrix} \qquad \begin{pmatrix} -\bar{K}^\circ \\ K^- \end{pmatrix}$$

$$T(\Xi^- K^+) = \frac{1}{2}(T_s^1 - T_s^\circ) = \frac{1}{2}(T_u^1 - T_u^\circ)$$

$$T(\Xi^\circ K^\circ) = \frac{1}{2}(T_s^1 + T_s^\circ) = -T_u^1$$

$$T(\Xi^- K^\circ) = T_s^1 = -\frac{1}{2}(T_u^1 + T_u^\circ)$$

Here the subscripts refer to the channel in which the isospin is being evaluated, and the superscripts refer to the total isotopic spin in that channel.

Table 1a. Legendre Polynomial Coefficients

	A_0	A_1	A_2	A_3	A_4	A_5	A_6	A_7	A_8	A_9	A_{10}	A_{11}	A_{12}	A_{13}
S_1S_1+P_1P_1	1													
S_1P_1		2.000												
S_1P_3+P_1D_3		4.000												
P_1P_3+S_1D_3			4.000											
P_3P_3+D_3D_3	2		2.000											
P_3D_3		0.800		7.200										
S_1D_5+P_1F_5			6.000											
P_1D_5+S_1F_5				6.000										
P_3D_5+D_3F_5		7.200		4.800										
D_3D_5+P_3F_5			1.714		10.286									
D_5D_5+F_5F_5	3		3.429		2.571									
D_5F_5		0.514		3.200		14.286								
S_1F_7+P_1G_7				8.000										
P_1F_7+S_1G_7					8.000									
P_3F_7+D_3G_7			10.286		5.714									
D_3F_7+P_3G_7				2.667		13.333								
D_5F_7+F_5G_7		10.286		8.000		5.714								
F_5F_7+D_5G_7			1.143		4.675		18.182							
F_7F_7+G_7G_7	4		4.762		4.208		3.030							
F_7G_7		0.381		2.182		6.593		22.844						
S_1G_9+P_1H_9					10.000									
P_1G_9+S_1H_9						10.000								
P_3G_9+D_3H_9				13.333		6.667								
D_3G_9+P_3H_9					3.636		16.364							
D_5G_9+F_5H_9			14.286		9.351		6.364							
F_5G_9+D_5H_9				1.818		6.154		22.028						
F_7G_9+G_7H_9		13.333		10.909		9.231		6.527						
G_7G_9+F_7H_9			0.866		3.237		8.485		27.413					
G_9G_9+H_9H_9	5		6.061		5.664		4.848		3.427					
G_9H_9		0.303		1.678		4.615		10.750		32.653				
S_1H_{11}+P_1I_{11}						12.000								
P_1H_{11}+S_1I_{11}							12.000							
P_3H_{11}+D_3I_{11}					16.364		7.636							
D_3H_{11}+P_3I_{11}						4.615		19.385						
D_5H_{11}+F_5I_{11}				18.182		10.769		7.049						
F_5H_{11}+D_5I_{11}					2.517		7.636		25.846					
F_7H_{11}+G_7I_{11}			18.182		12.587		10.182		7.049					
G_7H_{11}+F_7I_{11}				1.399		4.308		10.366		31.928				
G_9H_{11}+H_9I_{11}		16.364		13.706		12.308		10.366		7.256				
H_9H_{11}+G_9I_{11}			0.699		2.517		5.989		12.985		37.809			
$H_{11}H_{11}$+$I_{11}I_{11}$	6		7.343		7.049		6.417		5.410		3.781			
$H_{11}I_{11}$		0.252		1.371		3.620		7.638		15.549		43.570		
S_1I_{13}+P_1J_{13}							14.000							
P_1I_{13}+S_1J_{13}								14.000						
P_3I_{13}+D_3J_{13}						19.385		8.615						
D_3I_{13}+P_3J_{13}							5.600		22.400					
D_5I_{13}+F_5J_{13}					22.028		12.218		7.754					
F_5I_{13}+D_5J_{13}						3.231		9.122		29.647				
F_7I_{13}+G_7J_{13}				22.844		14.359		11.195		7.602				
G_7I_{13}+F_7J_{13}					1.958		5.390		12.243		36.409			
G_9I_{13}+H_9J_{13}			22.028		15.664		13.476		11.130		7.702			
H_9I_{13}+G_9J_{13}				1.142		3.379		7.365		15.204		42.910		
$H_{11}I_{13}$+$I_{11}J_{13}$		19.385		16.448		15.204		13.640		11.403		7.922		
$I_{11}I_{13}$+$H_{11}J_{13}$			0.587		2.073		4.728		9.275		18.083		49.253	
$I_{13}I_{13}$+$J_{13}J_{13}$	7		8.615		8.397		7.881		7.085		5.918		4.104	
$I_{13}J_{13}$		0.215		1.161		3.001		6.062		11.155		20.914		55.492

Table 1b. Legendre Polynomial Coefficients

	B_1	B_2	B_3	B_4	B_5	B_6	B_7	B_8	B_9	B_{10}	B_{11}	B_{12}	B_{13}
$-S_1P_1$	2.000												
$S_1P_3-P_1D_3$	2.000												
$P_1P_3-S_1D_3$		2.000											
$-P_3D_3$	1.600		2.400										
$S_1D_5-P_1F_5$		2.000											
$P_1D_5-S_1F_5$			2.000										
$P_3D_5-D_3F_5$	3.600		0.400										
$D_3D_5-P_3F_5$		1.429		2.571									
$-D_5F_5$	1.543		1.600		2.857								
$S_1F_7-P_1G_7$			2.000										
$P_1F_7-S_1G_7$				2.000									
$P_3F_7-D_3G_7$		3.429		0.571									
$D_3F_7-P_3G_7$			1.333		2.667								
$D_5F_7-F_5G_7$	5.143		0.667		0.190								
$F_5F_7-D_5G_7$		1.333		1.636		3.030							
$-F_7G_7$	1.524		1.455		1.758		3.263						
$S_1G_9-P_1H_9$				2.000									
$P_1G_9-S_1H_9$					2.000								
$P_3G_9-D_3H_9$			3.333		0.667								
$D_3G_9-P_3H_9$				1.273		2.727							
$D_5G_9-F_5H_9$		4.762		0.935		0.303							
$F_5G_9-D_5H_9$			1.212		1.641		3.147						
$F_7G_9-G_7H_9$	6.667		0.909		0.308		0.117						
$G_7G_9-F_7H_9$		1.299		1.457		1.818		3.427					
$-G_9H_9$	1.515		1.399		1.538		1.920		3.628				
$S_1H_{11}-P_1I_{11}$					2.000								
$P_1H_{11}-S_1I_{11}$						2.000							
$P_3H_{11}-D_3I_{11}$				3.273		0.727							
$D_3H_{11}-P_3I_{11}$					1.231		2.769						
$D_5H_{11}-F_5I_{11}$			4.545		1.077		0.378						
$F_5H_{11}-D_5I_{11}$				1.133		1.636		3.231					
$F_7H_{11}-G_7I_{11}$		6.061		1.259		0.485		0.196					
$G_7H_{11}-F_7I_{11}$			1.166		1.436		1.851		3.548				
$G_9H_{11}-H_9I_{11}$	8.182		1.142		0.410		0.185		0.081				
$H_9H_{11}-G_9I_{11}$		1.282		1.385		1.569		1.984		3.781			
$-H_{11}I_{11}$	1.510		1.371		1.448		1.637		2.073		3.961		
$S_1I_{13}-P_1J_{13}$						2.000							
$P_1I_{13}-S_1J_{13}$							2.000						
$P_3I_{13}-D_3I_{13}$					3.231		0.769						
$D_3I_{13}-P_3J_{13}$						1.200		2.800					
$D_5I_{13}-F_5J_{13}$				4.406		1.164		0.431					
$F_5I_{13}-D_5J_{13}$					1.077		1.629		3.294				
$F_7I_{13}-G_7J_{13}$			5.711		1.436		0.600		0.253				
$G_7I_{13}-F_7J_{13}$				1.077		1.412		1.870		3.641			
$G_9I_{13}-H_9J_{13}$		7.343		1.566		0.642		0.309		0.140			
$H_9I_{13}-G_9J_{13}$			1.142		1.351		1.578		2.027		3.901		
$H_{11}I_{13}-I_{11}J_{13}$	9.692		1.371		0.507		0.244		0.127		0.060		
$I_{11}I_{13}-H_{11}J_{13}$		1.273		1.348		1.464		1.675		2.137		4.104	
$-I_{13}J_{13}$	1.508		1.355		1.400		1.515		1.735		2.218		4.269

III. DATA PROCESSING

The film of 2.1 and 2.64 GeV/c K^- on deuterium was scanned for all one-prong events (a spectator proton does not count as a prong) with either one or two associated vees. These events were measured on a Franckenstein measuring machine and kinematically fitted with the program SIOUX. Failing events were re-scanned and remeasured at least once, and up to four times. For our final sample we chose those events with a visible spectator and momentum less than 300 MeV/c. We have 93 such events at 2.1 GeV/c, and 46 at 2.64 GeV/c. (Events with high momentum spectators are presumably due to interactions off the entire deuteron rather than off the neutron.)

At 2.1 GeV/c three scans were carried out. About 25% of the events were scanned twice, and about 10% were scanned three times. The scanning efficiencies were estimated from the formula $e_a = N_{ab}/N_b$, where e_a is the efficiency for scan #a, N_{ab} is the number of events found on both scans #a and #b, and N_b is the number of events found on scan #b. The scanning efficiencies estimated in this way were 83%, 55%, and 83% for scans 1, 2, and 3 respectively. The overall scanning efficiency for the three scans combined is 86%.

There are two scanning biases (which presumably reflect in the above efficiencies) which could affect our production distributions. The first is due to the loss of Ξ's that decay forward in the laboratory. Weighting factors to correct for such as loss (and for the loss of short Ξ and Λ decays) were calculated for the reaction $K^- p \to \Xi^- K^+$.[3] By studying the effect of removing these weights on the Legendre expansion coefficients

(see Figure 1) we determined that with our limited statistics such losses did not significantly bias our data.

The second and potentially more serious bias comes from the loss of events with no visible difference between the incident K^- and the Ξ^- directions. (A scanner would call such an event a V-one-prong.) Such a bias would result in a depletion of events in the $\cos\theta \approx -1$ direction. This bias presumably would not be as serious in the subset of events that had either a visible K° decay (which points back to the production vertex) or a visible spectator proton. We compared the angular distributions of these subsets, and we did not see any significant differences. The statistics after the cuts were very poor, however, and we decided to increase our error estimates in order to account for a possible bias. If the Ξ's in the region $-1 \lesssim \cos\theta \lesssim -0.8$ were detected with only 1/3 efficiency, our total cross sections would be about one standard deviation greater than the present estimate, and the calculated Legendre coefficients A_L/A_0 and B_L/A_0 would be shifted by approximately one standard deviation (see Figure 2). To account for the possible bias we doubled the upper errors for the total cross sections and we doubled all the errors for the Legendre coefficients.

The total cross sections are presented in the following table:

Lab. Mom.	Events with Visible Λ	Path Length	Missed $\Lambda\to n\pi^\circ$ Correction	Avg. Wt. for Decay and Scanning Losses	Total Cross Section
2.1	93	2.71 ev/μb	1.53	1.3	69^{+14}_{-7} μb
2.64	46	2.84 ev/μb	1.53	1.45	36^{+10}_{-5} μb

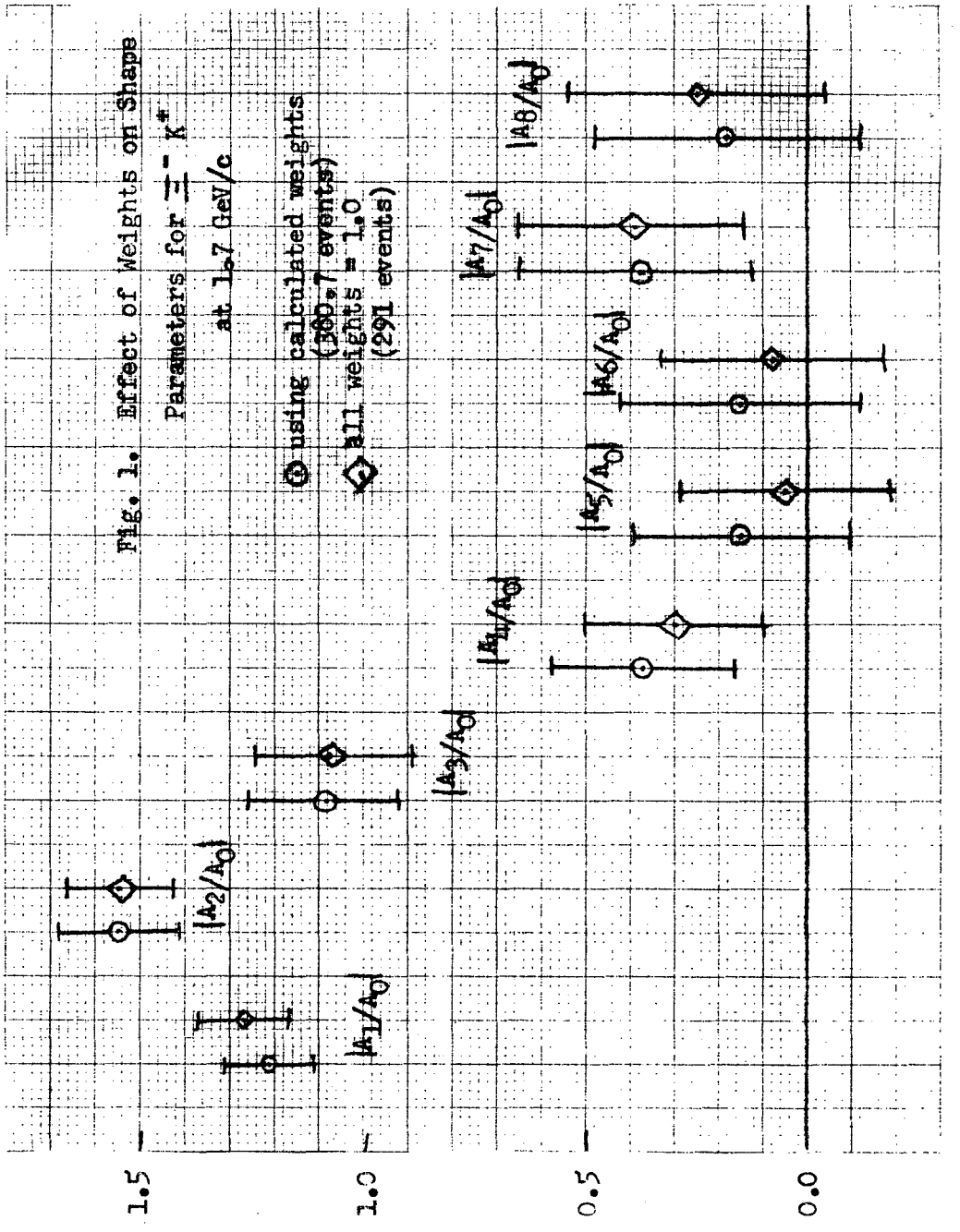
Fig. 1. Effect of Weights on Shape Parameters for $\Xi^- K^+$ at 1.7 GeV/c
using calculated weights (360.7 events)
all weights = 1.0 (291 events)
$|A_1/A_0|$
$|A_2/A_0|$
$|A_3/A_0|$
$|A_4/A_0|$
$|A_5/A_0|$
$|A_6/A_0|$
$|A_7/A_0|$
$|A_8/A_0|$
1.5
1.0
0.5
0.0

Figure 1

The differential cross sections and polarization distributions are shown in Figures 3 and 4. The polarizations were calculated by using the complete distribution function for the sequential decay $\Xi \to \Lambda\pi$, $\Lambda \to p\pi^-$.[3]

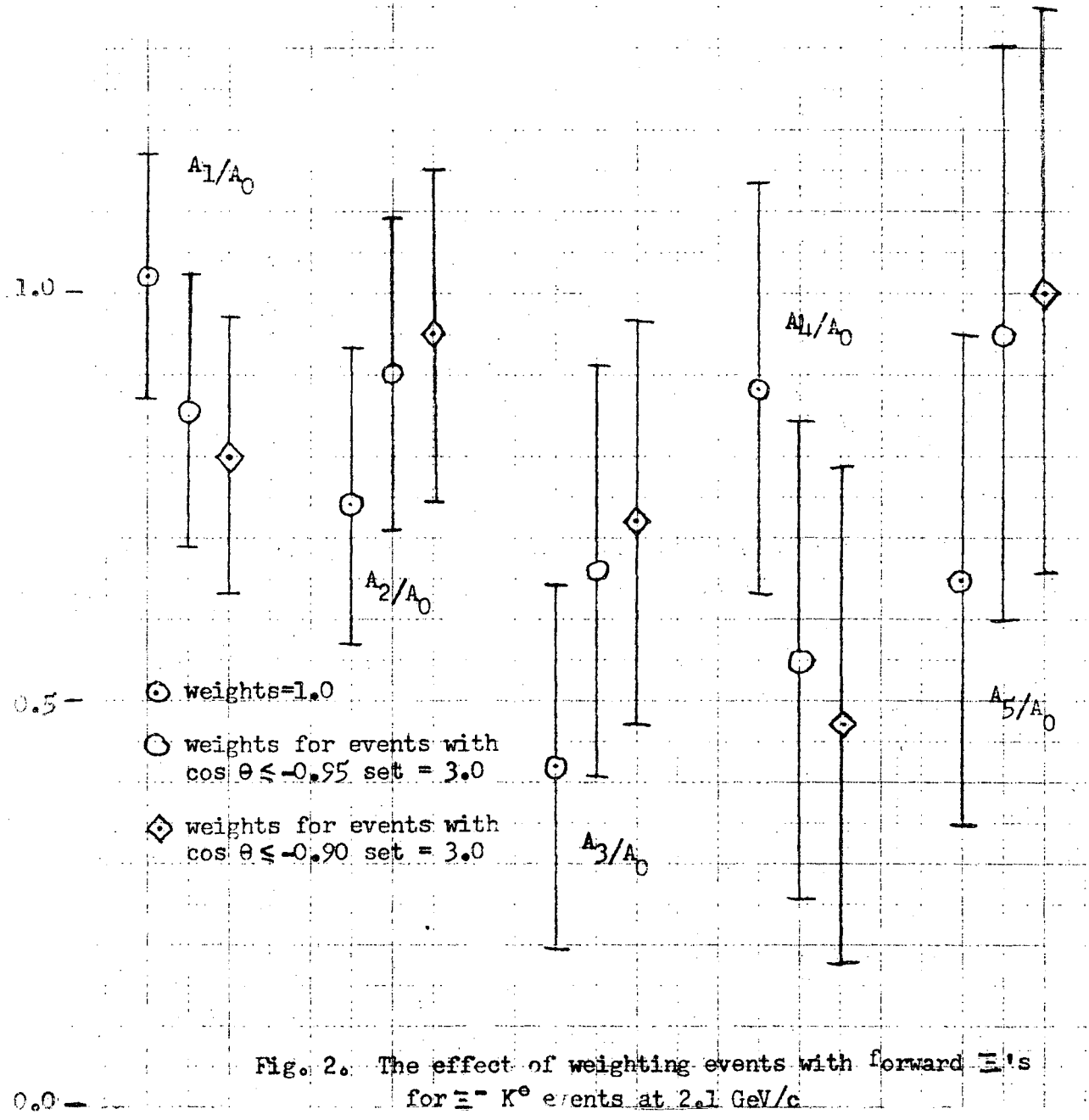

Fig. 2. The effect of weighting events with forward Ξ's for $\Xi^- K^0$ events at 2.1 GeV/c

FIGURE 2

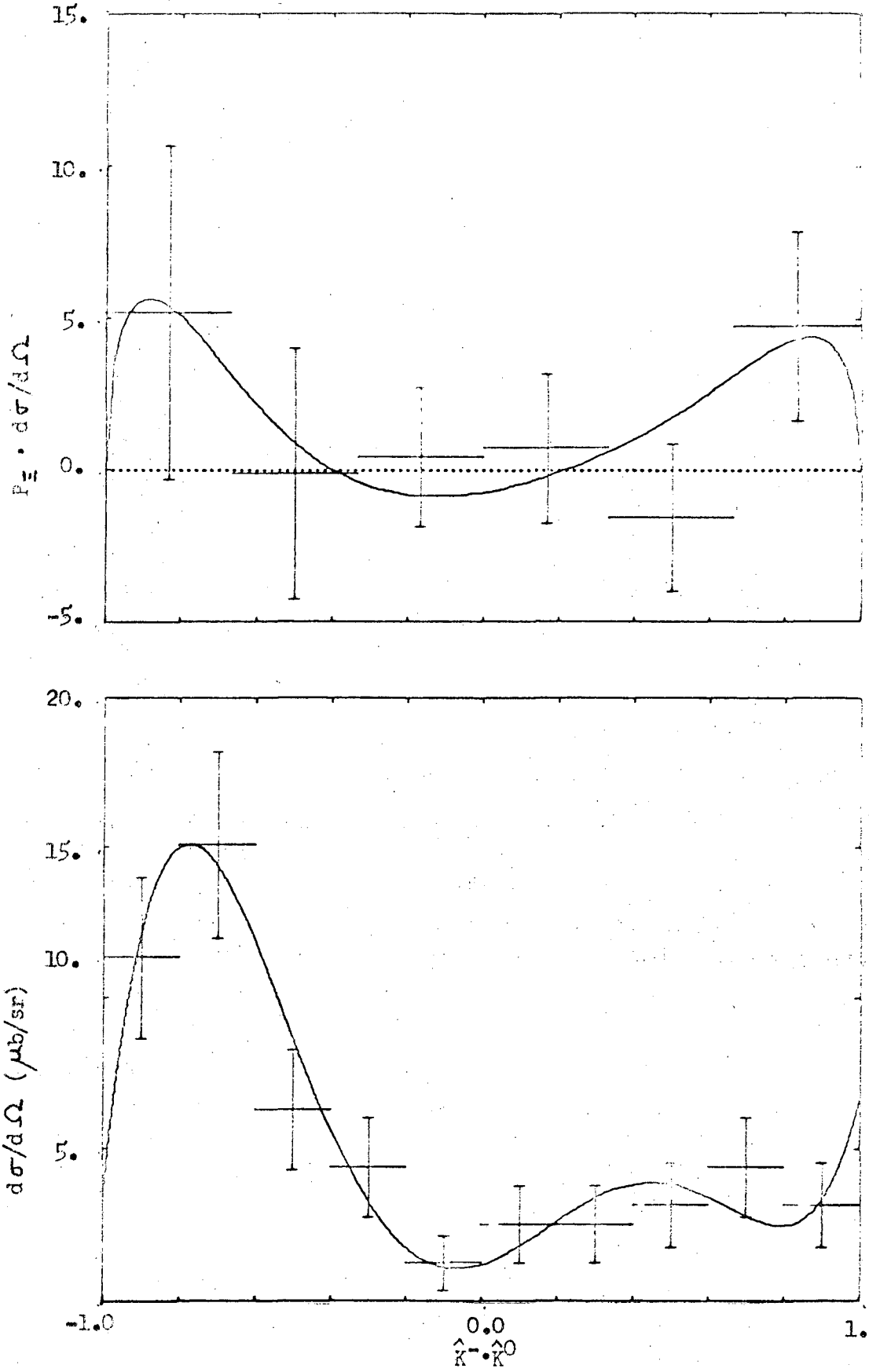

Figure 3. Production distributions for $K^-n \to \Xi^- K^0$ at 2.1 GeV/c. The curves are calculated from the Legendre function moments with $l_{max}=5$.

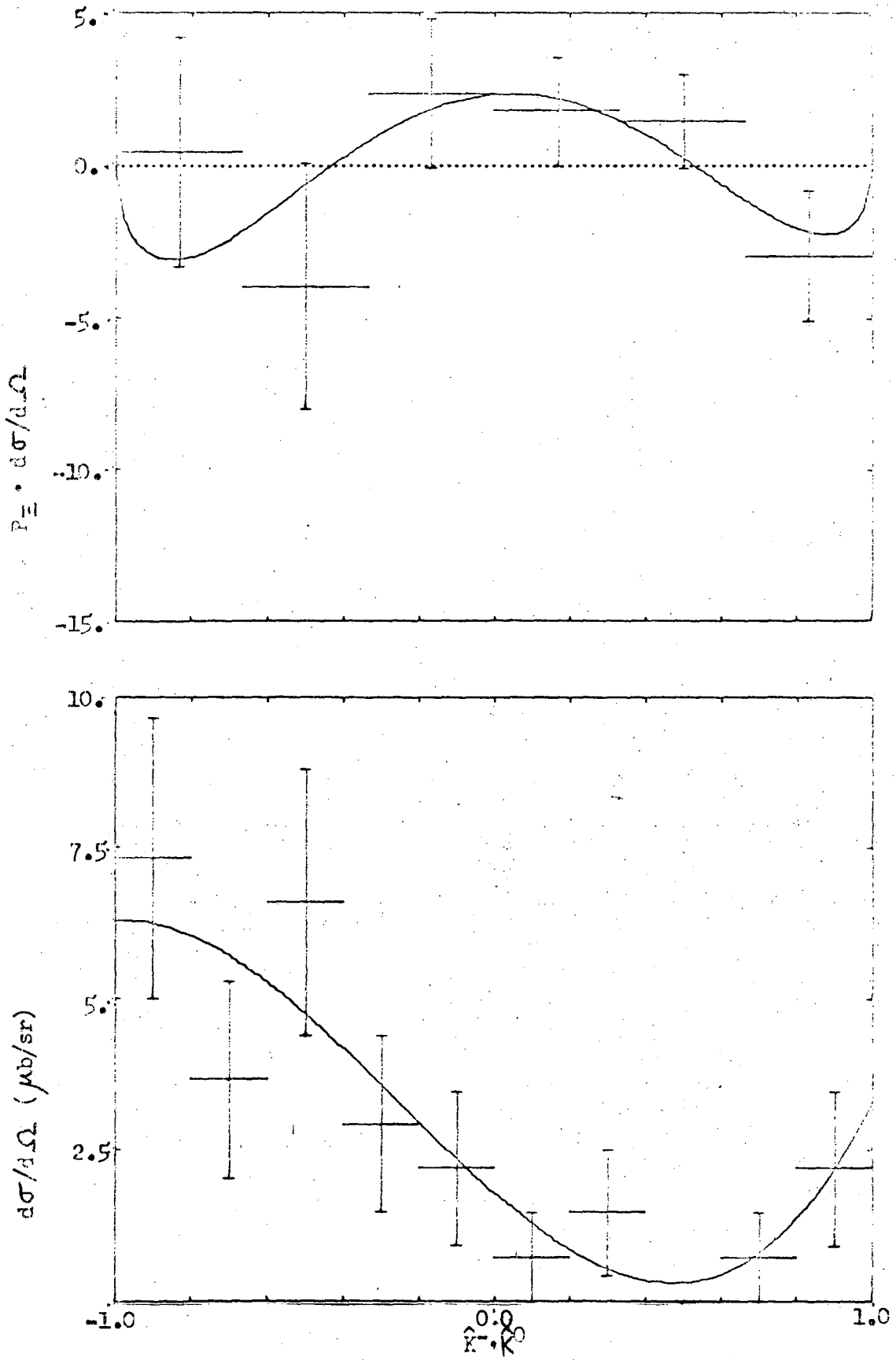

Figure 4. Production distributions for $K^-n \rightarrow \Xi^- K^0$ at 2.64 GeV/c. The curves are calculated from the Legendre function moments with $L_{max}=3$.

IV. THE DATA

A. Qualitative Features

Figures 3 - 7 show the differential cross section and polarization distributions for our reactions at selected energies. Except for the deuterium data, these distributions have been published previously.[1-4] The major features of the data are summarized below:

1. A strong peak in the backward direction in reactions (1) and (3), at all beam momenta above 1.22 GeV/c.
2. The backward peak sharpens considerably at the higher energies.
3. At 2.64 GeV/c there are rapid undulations in the differential cross section. (A_1 through A_8 are all more than two standard deviations from zero.)
4. The total cross section in reaction (2), $K^- p \to \Xi^\circ K^\circ$ is considerably smaller than that for the other two reactions.
5. The shape of the distributions in reaction (2) varies rapidly with energy.
6. There is significant polarization present at most energies. The polarization in the region of the backward peak is low, and there is a region ($0.0 < \cos\theta < 0.8$) where the polarization is consistent with -1.

$A_0 = \sigma/4\pi\lambda^2$ is shown in Figure 8 and Table 6. In both reactions (1) and (2) it peaks at about 1.7 GeV/c and then falls off. The A_ℓ's and B_ℓ's are shown in Figures 9 - 16 and Tables 2 - 5. In reaction (1) only A_ℓ's and B_ℓ's through $\ell = 3$ are significantly different from zero at the lower energies. A_6 is 3-1/2 standard deviations from zero at

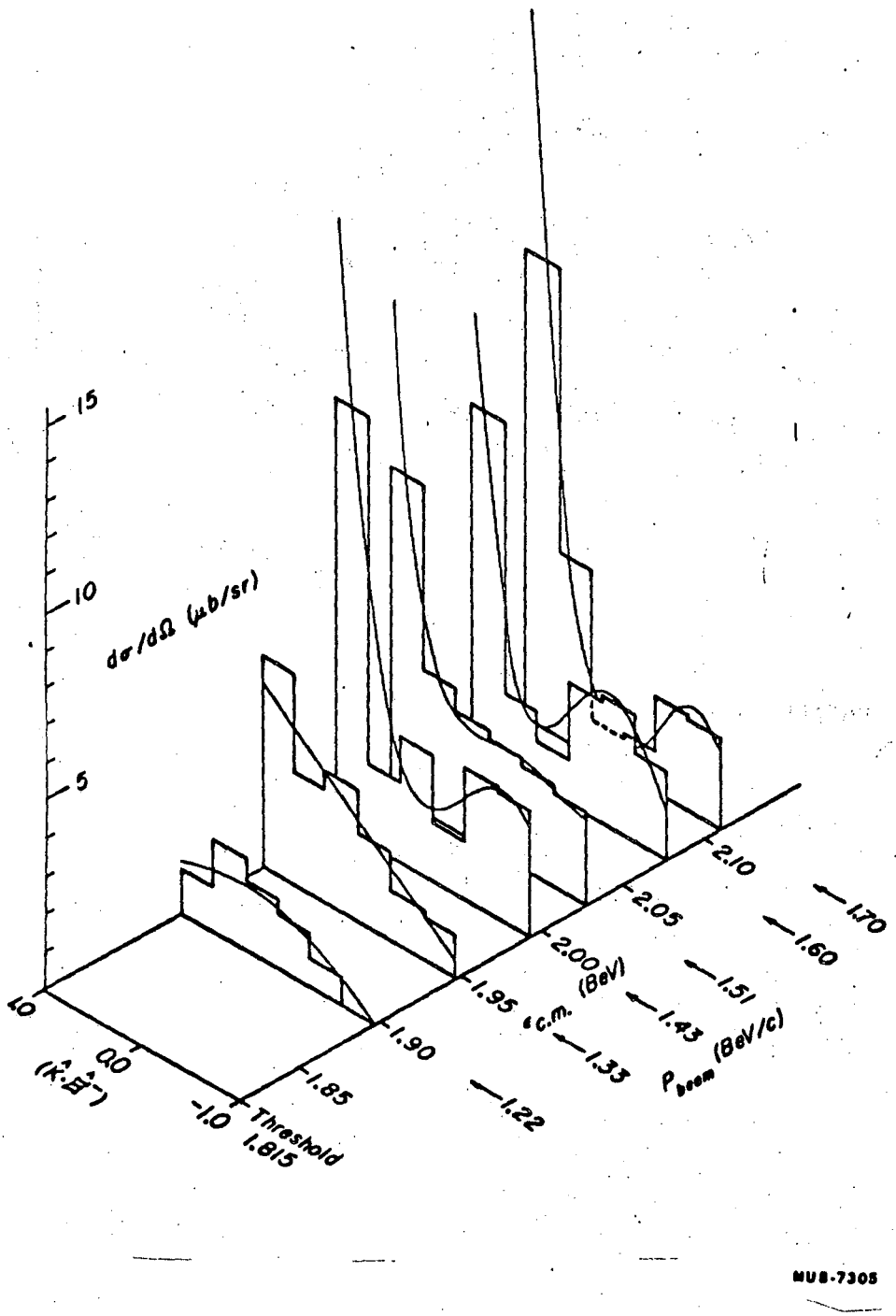

FIGURE 5

Ξ^- K^+ differential cross-sections from 1.22 to 1.70 GeV/c

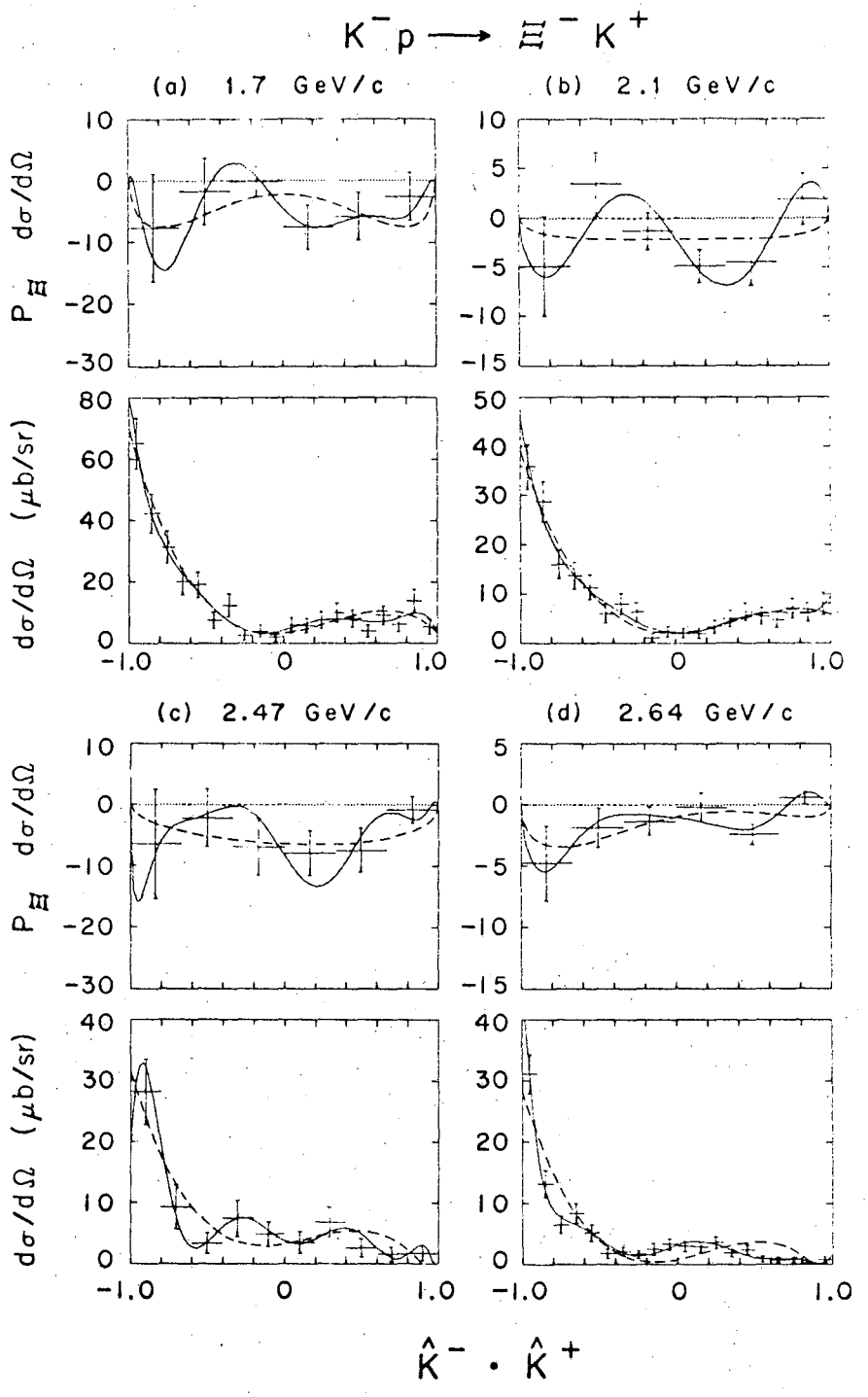

Figure 6. Production distributions for $K^- p \rightarrow \Xi^- K^+$ from 1.7 to 2.64 GeV/c. The solid curves are calculated from Legendre function moments of the distributions with L_{max} = 7, 6, 8, and 8 at the respective momenta. Dashed curves corresponding to L_{max}=3 are also plotted.

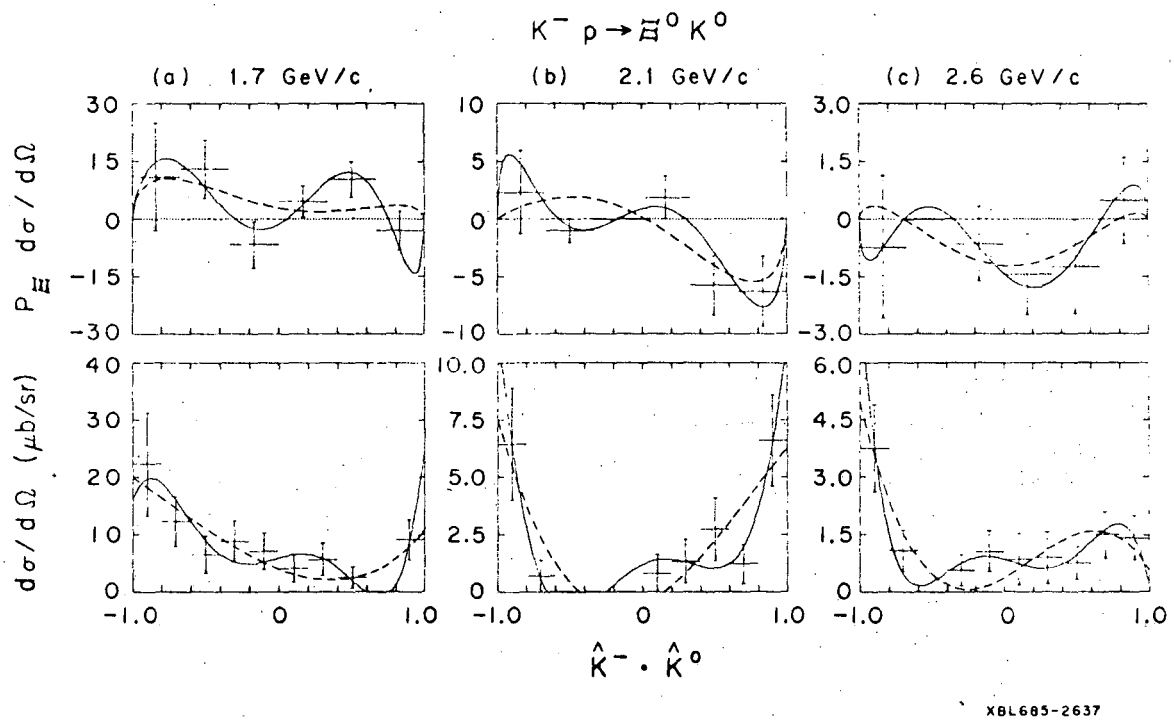

Figure 7. Production distributions for $K^- p \to \Xi^0 K^0$ from 1.7 to 2.64 GeV/c. The solid curves are calculated from Legendre function moments of the distributions with $L_{max}=5$; the dashed curves correspond to $L_{max}=3$.

A_L/A_0 for $K^- p \rightarrow \Xi^- K^+$

P_{lab}	L = 1	2	3	4	5	6	7	8
1.22	-.68 ± .24	-.46 ± .34	.56 ± .41	-.21 ± .49	.40 ± .46	.04 ± .50	.32 ± .63	.37 ± .63
1.33	-.95 ± .17	.23 ± .25	-.15 ± .30	.02 ± .37	-.57 ± .43	.18 ± .45	-.27 ± .49	.71 ± .50
1.43	-.81 ± .18	.87 ± .23	-1.17 ± .26	.26 ± .31	.38 ± .35	-.02 ± .38	.30 ± .41	-.38 ± .42
1.51	-.83 ± .09	.77 ± .12	-.60 ± .14	.10 ± .16	-.08 ± .17	-.20 ± .19	.16 ± .20	-.07 ± .22
1.60	-1.00 ± .17	1.18 ± .22	-1.36 ± .25	.38 ± .30	.07 ± .32	-.18 ± .37	.16 ± .41	-.50 ± .43
1.70	-1.34 ± .24	1.56 ± .31	-1.24 ± .43	.31 ± .55	-.08 ± .63	1.09 ± .65	-1.04 ± .72	1.41 ± .75
1.70	-1.22 ± .11	1.55 ± .14	-1.08 ± .18	.37 ± .21	-.15 ± .24	.16 ± .26	-.38 ± .28	-.18 ± .30
1.80	-.96 ± .23	1.99 ± .22	-1.06 ± .31	.16 ± .37	.01 ± .42	-.89 ± .46	-.08 ± .48	-.61 ± .50
1.95	-.64 ± .26	1.19 ± .29	-1.25 ± .35	.06 ± .41	-.13 ± .48	-.03 ± .51	.15 ± .55	-.81 ± .57
2.00	-1.00 ± .10	1.56 ± .11	-.83 ± .16	.13 ± .18	-.38 ± .21	.71 ± .22	-.38 ± .23	.28 ± .24
2.10	-1.05 ± .11	1.50 ± .13	-.79 ± .18	.24 ± .20	-.17 ± .22	.34 ± .24	.08 ± .27	-.38 ± .29
2.47	-1.29 ± .19	1.02 ± .31	-1.25 ± .33	.70 ± .36	-.12 ± .43	-.50 ± .46	.91 ± .52	-1.30 ± .55
2.64	-1.64 ± .09	1.60 ± .15	-1.82 ± .18	1.54 ± .22	-.84 ± .25	.84 ± .27	-1.00 ± .30	.70 ± .32

Table 2. Legendre expansion coefficients for $K^- p \rightarrow \Xi^- K^+$

B_T/A_0 for $K^- p \rightarrow \Xi^- K^+$

P_{lab}	L = 1	2	3	4	5	6	7	8
1.22	.52 ± .52	-.69 ± .35	.23 ± .36	-.02 ± .32	.10 ± .31	-.18 ± .26	-.01 ± .21	.03 ± .20
1.33	.84 ± .32	-.55 ± .22	-.15 ± .19	-.06 ± .18	.14 ± .15	.01 ± .16	.15 ± .14	-.12 ± .14
1.43	.01 ± .25	-.76 ± .17	.02 ± .17	-.10 ± .15	.11 ± .14	-.09 ± .13	.09 ± .12	-.08 ± .12
1.51	.00 ± .13	-.47 ± .11	-.02 ± .10	.06 ± .09	.01 ± .08	.04 ± .07	-.12 ± .07	-.04 ± .06
1.60	-.36 ± .26	-.02 ± .24	-.18 ± .21	.12 ± .18	.03 ± .17	-.01 ± .15	.15 ± .14	-.00 ± .13
1.70	-.83 ± .31	.19 ± .33	-.44 ± .25	.29 ± .22	.03 ± .21	.36 ± .21	-.26 ± .18	.01 ± .16
1.70	-.38 ± .15	-.00 ± .14	-.15 ± .13	.12 ± .12	.00 ± .11	-.08 ± .10	.07 ± .09	-.05 ± .08
1.80	-.64 ± .29	-.29 ± .31	-.34 ± .29	-.03 ± .24	-.05 ± .20	-.23 ± .18	.12 ± .18	.02 ± .18
1.95	-.32 ± .33	-.33 ± .29	-.27 ± .27	.34 ± .26	-.03 ± .22	.17 ± .21	.24 ± .19	-.04 ± .17
2.00	-.47 ± .11	-.03 ± .12	-.21 ± .10	.17 ± .09	.11 ± .08	-.01 ± .08	.12 ± .07	-.09 ± .07
2.10	-.26 ± .15	0. ± .14	-.02 ± .12	.24 ± .10	.02 ± .10	-.05 ± .09	.12 ± .08	-.09 ± .07
2.47	-.91 ± .32	-.03 ± .29	-.01 ± .25	.37 ± .20	-.21 ± .18	-.03 ± .17	-.05 ± .17	.11 ± .15
2.64	-.37 ± .15	.18 ± .12	-.12 ± .11	.17 ± .10	-.02 ± .10	-.00 ± .09	-.00 ± .08	-.03 ± .08

TABLE 3

Legendre expansion coefficients for $K^- p \rightarrow \Xi^- K^+$

A_L/A_0 and B_L/A_0 for $K^- p \rightarrow \Xi^0 K^0$

	P_{lab}	L = 1	2	3	4	5	6	7	8
A_L/A_0	1.51	-.77 ± .22	1.64 ± .25	.24 ± .35	.56 ± .38	.36 ± .44	-.20 ± .47	-.56 ± .52	-.34 ± .55
	1.70	-.86 ± .30	.95 ± .41	.27 ± .51	.63 ± .55	1.14 ± .58	.20 ± .63	.98 ± .65	-.36 ± .69
	2.00	.58 ± .38	1.98 ± .40	.29 ± .61	1.00 ± .66	.36 ± .80	.56 ± .87	-1.06 ± .92	-.09 ± .93
	2.10	.36 ± .47	2.48 ± .46	-.68 ± .81	2.26 ± .79	.07 ± .95	2.20 ± .99	-.09 ±1.13	.50 ±1.15
	2.64	-.42 ± .35	1.36 ± .43	-1.45 ± .47	1.05 ± .56	-1.40 ± .61	-.42 ± .66	.06 ± .67	-.24 ± .72
B_L/A_0	1.51	.50 ± .25	-.31 ± .25	.51 ± .23	-.40 ± .20	.20 ± .18	-.24 ± .18	-.05 ± .17	-.16 ± .16
	1.70	.75 ± .41	-.30 ± .34	.23 ± .31	-.48 ± .29	-.30 ± .27	.22 ± .26	-.03 ± .24	.04 ± .23
	2.00	.42 ± .42	-.52 ± .45	-.04 ± .41	-.54 ± .34	-.38 ± .27	.26 ± .26	-.26 ± .26	.37 ± .28
	2.10	-.45 ± .50	-1.16 ± .44	-.37 ± .48	-.70 ± .50	.19 ± .52	-.51 ± .46	-.78 ± .43	-.21 ± .45
	2.64	-.63 ± .35	-.07 ± .31	.25 ± .30	.34 ± .27	-.10 ± .24	.33 ± .21	-.15 ± .20	.19 ± .20

TABLE 4

Legrendre expansion coefficients for $K^- p \rightarrow \Xi^0 K^0$

A_L/A_0 and B_L/A_0 for $K^- n \to \Xi^- K^0$

	P_{lab}	L= 1	2	3	4	5	6	7	8
A_L/A_0	1.51	-.65 ± .27	.40 ± .36	-.59 ± .38					
	2.10	-.94 ± .38	.87 ± .44	.17 ± .28	-.93 ± .63	1.05 ± .75	-.48 ± .81	.34 ± .86	.11 ± .96
	2.64	-1.10 ± .53	.72 ± .75	.56 ± .93	-.16 ± .98	.13 ± .54	.22 ± 1.25	-.03 ± 1.32	-.88 ± 1.26
B_L/A_0	2.10	-.27 ± .61	.01 ± .55	.33 ± .45	-.05 ± .37	.05 ± .30	-.18 ± .31	-.31 ± .30	-.18 ± .26
	2.64	.11 ± .88	.11 ± .69	-.49 ± .58	-.36 ± .50	.16 ± .43	.08 ± .36	-.13 ± .34	.56 ± .37

TABLE 5

Legendre expansion coefficients for $K^- n \to \Xi^- K^0$

Table 6. $A_0 = \sigma/4\pi\lambda^2$ (in units of 10^{-3})

P_{lab} (GeV/c)	$A_0(\Xi^-K^+)$	$A_0(\Xi^0K^0)$	$A_0(\Xi^-K^0)$
1.22	3.65 ± 0.7	2.40 ± 1.10	
1.33	8.74 ± 1.0	3.5 ± 1.6	
1.43	14.76 ± 1.9	3.2 ± 1.8	
1.51	14.79 ± 0.9	7.8 ± 1.1	16.5 ± 2.3
1.60	14.38 ± 2.0	9.8 ± 3.0	
1.7[a]	18.13 ± 2.0	13.2 ± 3.2	
1.7[b]	20.95 ± 1.9	11.7 ± 2.7	
1.80	16.64 ± 1.9	8.7 ± 2.4	
1.95	14.13 ± 2.0	11.1 ± 3.5	
2.0	15.15 ± 1.2		
2.1	17.43 ± 1.5	3.8 ± 1.1	10.4 ± 2.2
2.47	16.50 ± 2.6	4.5 ± 2.1	
2.64	12.0 ± 1.2	3.1 ± 0.8	7.2 ± 2.2

[a]Data from reference 1.

[b]Data from reference 3.

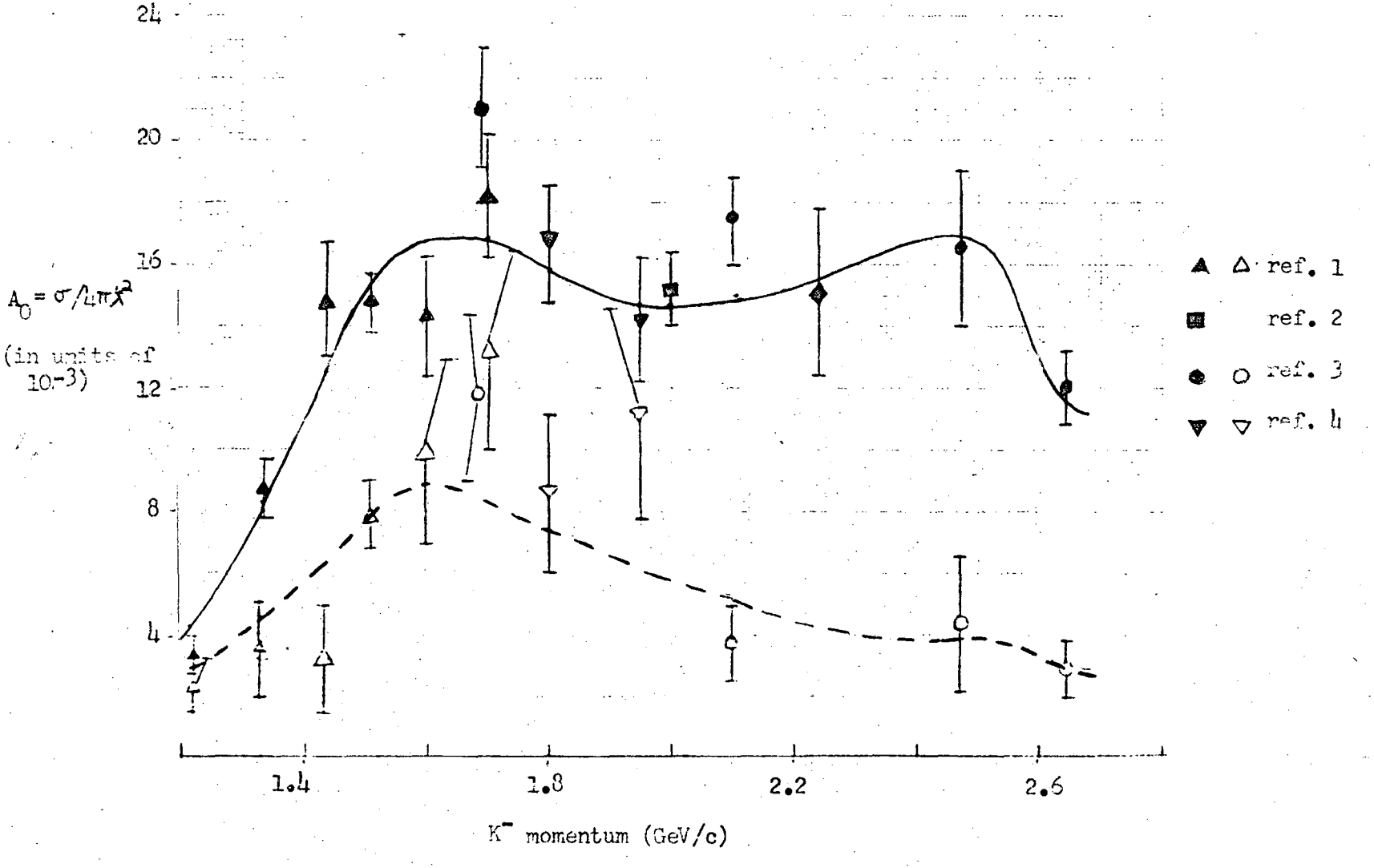

Figure 8. Total cross section divided by $4\pi\lambda^2$ for $K^-p \to \Xi^-K^+$ (solid symbols) and $K^-p \to \Xi^0K^0$ (open symbols) as a function of beam momentum. The curves correspond to the $\chi^2 = 372$ fit discussed in section V.

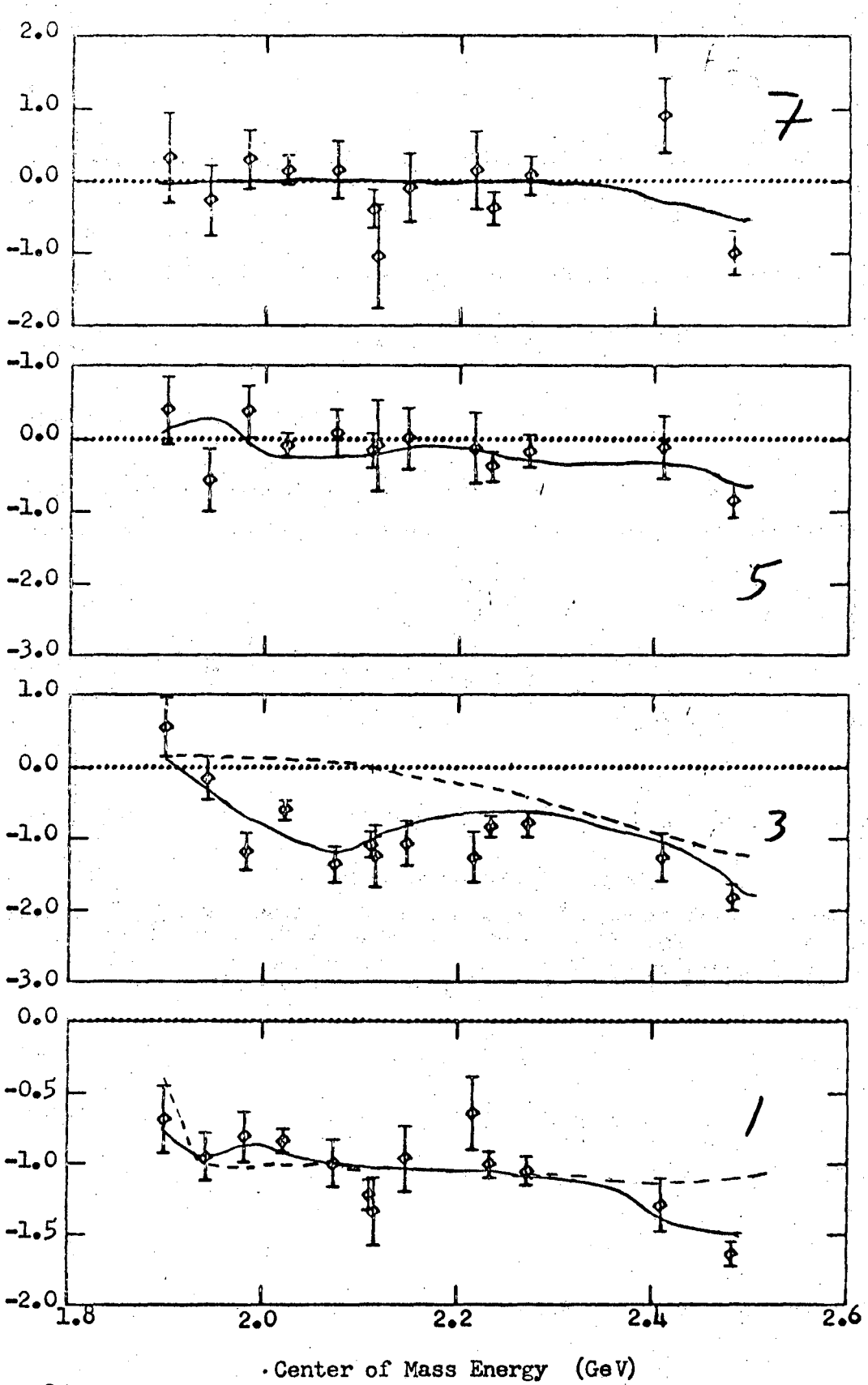

Figure 9. Legendre expansion coefficients. The solid curve corresponds to the $\chi^2 = 372$ solution discussed in section V. The dashed curves corresponds to the same fit when the amounts of all the resonances are set = 0.

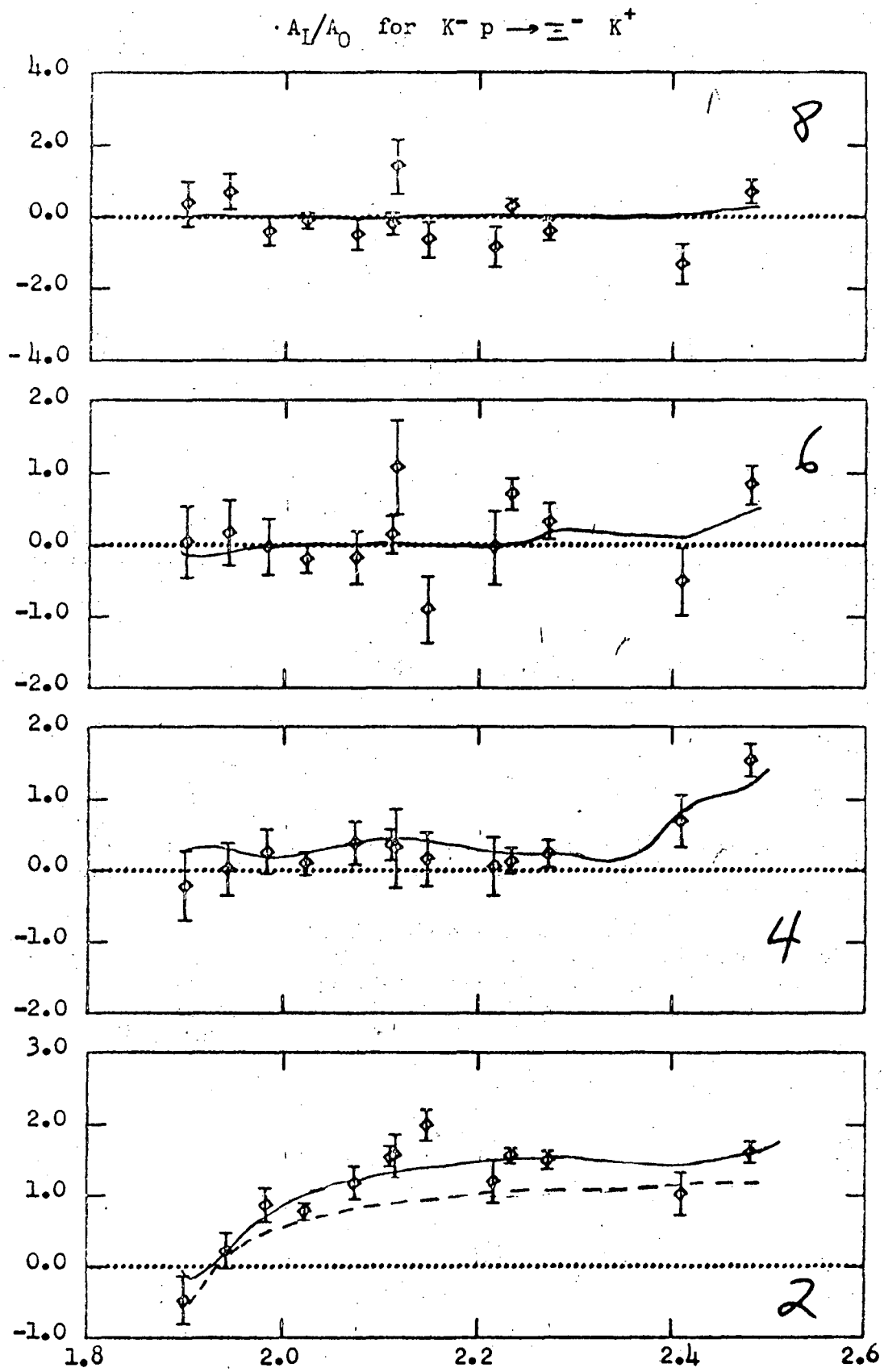

Figure 10. Legendre expansion coefficients. The solid curve corresponds to the $\chi^2 = 372$ solution discussed in section V. The dashed curves corresponds to the same fit when the amounts of all the resonances are set = 0.

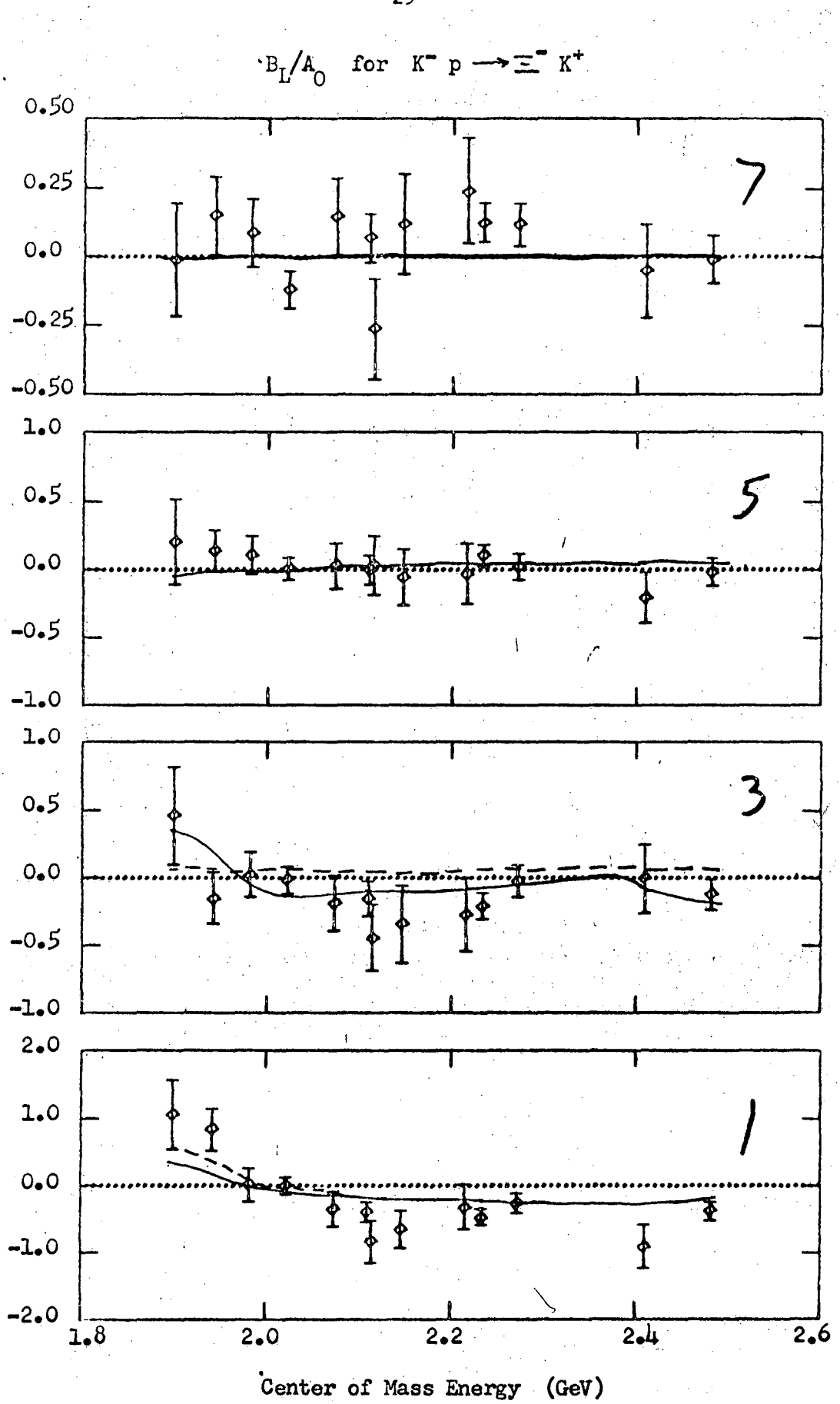

Figure 11. Legendre expansion coefficients. The solid curve corresponds to the $\chi^2 = 372$ solution discussed in section V. The dashed curves corresponds to the same fit when the amounts of all the resonances are set = 0.

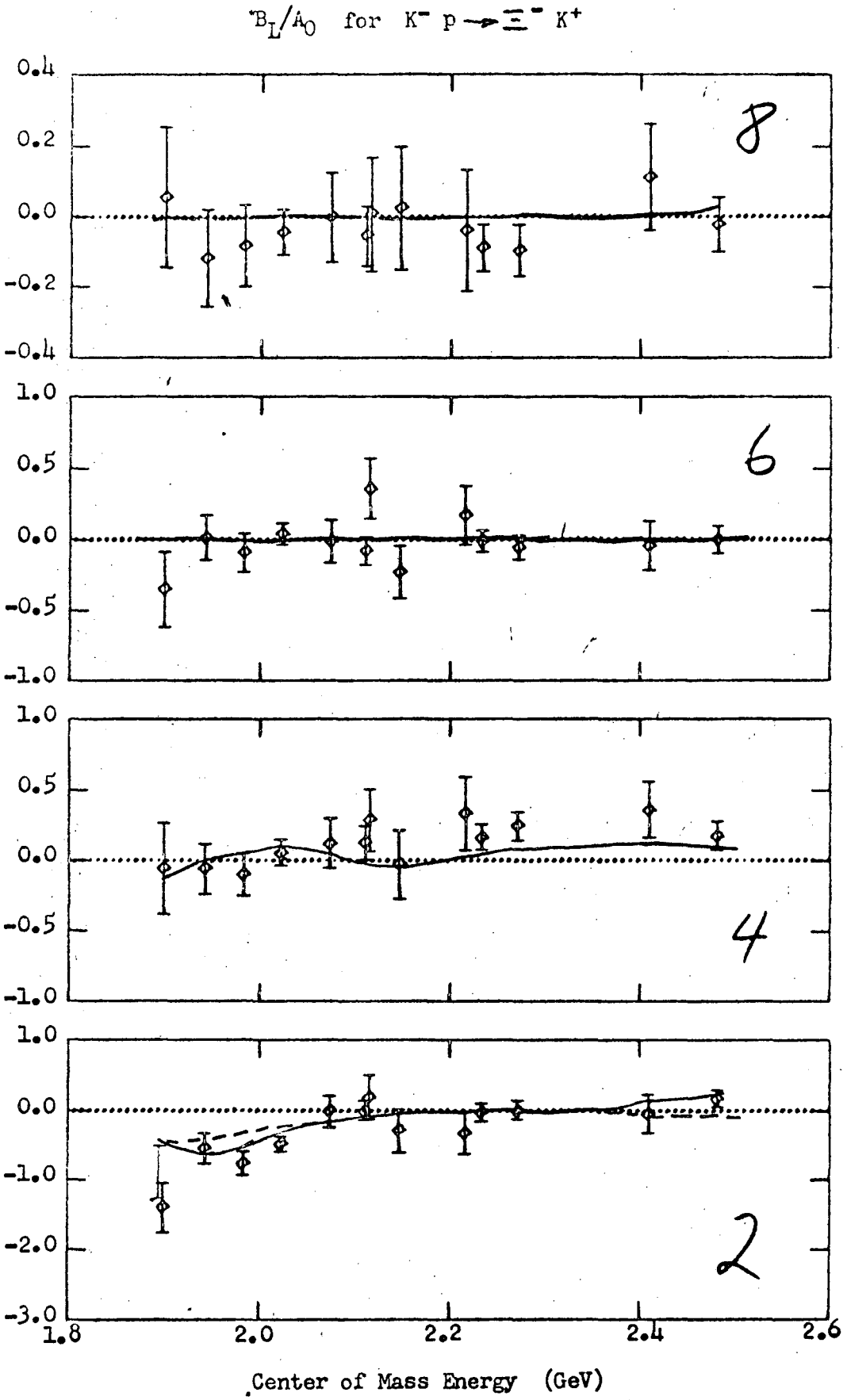

Figure12 . Legendre expansion coefficients. The solid curve corresponds to the $\chi^2 = 372$ solution discussed in section V. The dashed curves corresponds to the same fit when the amounts of all the resonances are set = 0.

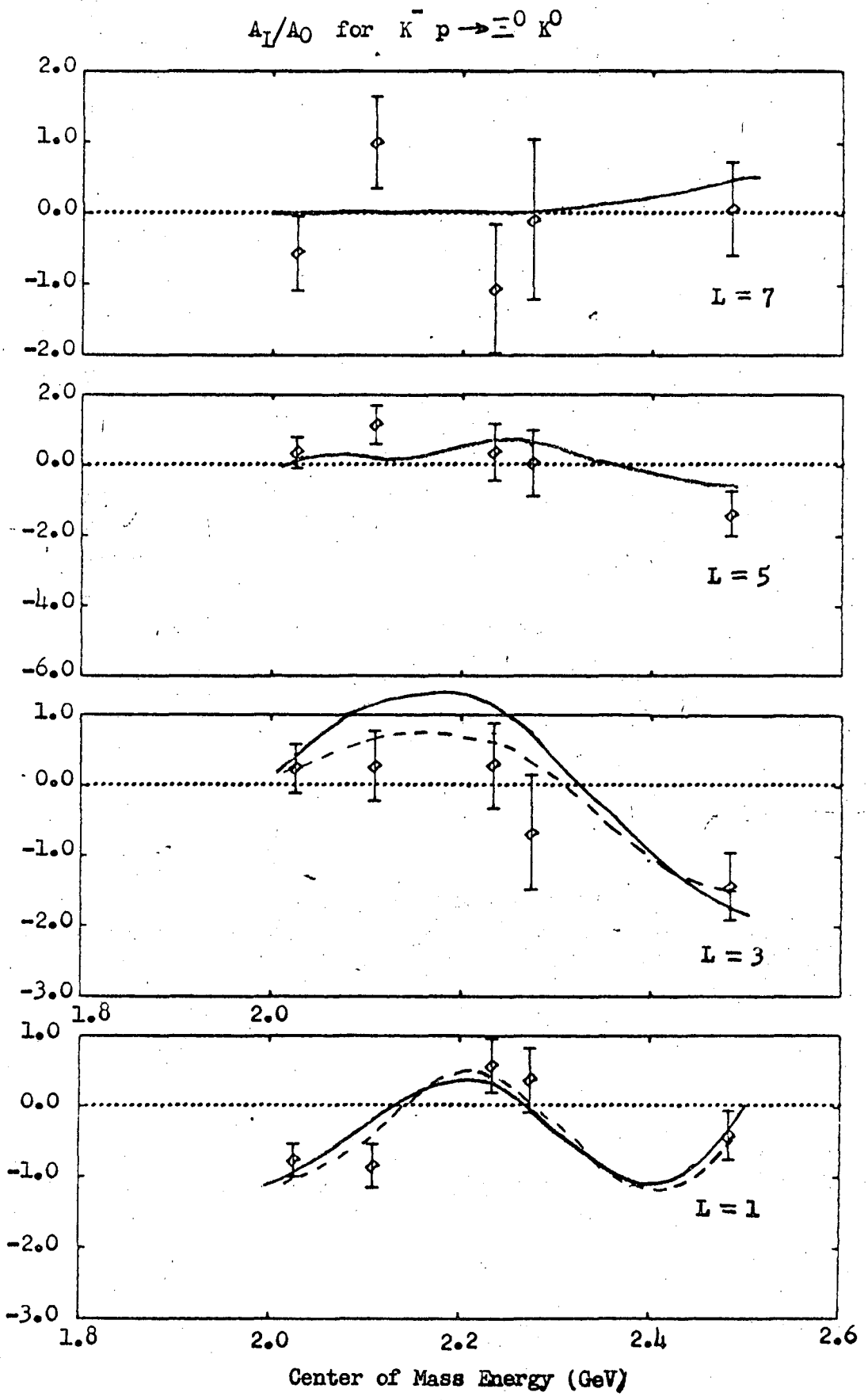

Figure 13. Legendre expansion coefficients. The solid curve corresponds to the $\chi^2 = 372$ solution discussed in section V. The dashed curves corresponds to the same fit when the amounts of all the resonances are set = 0.

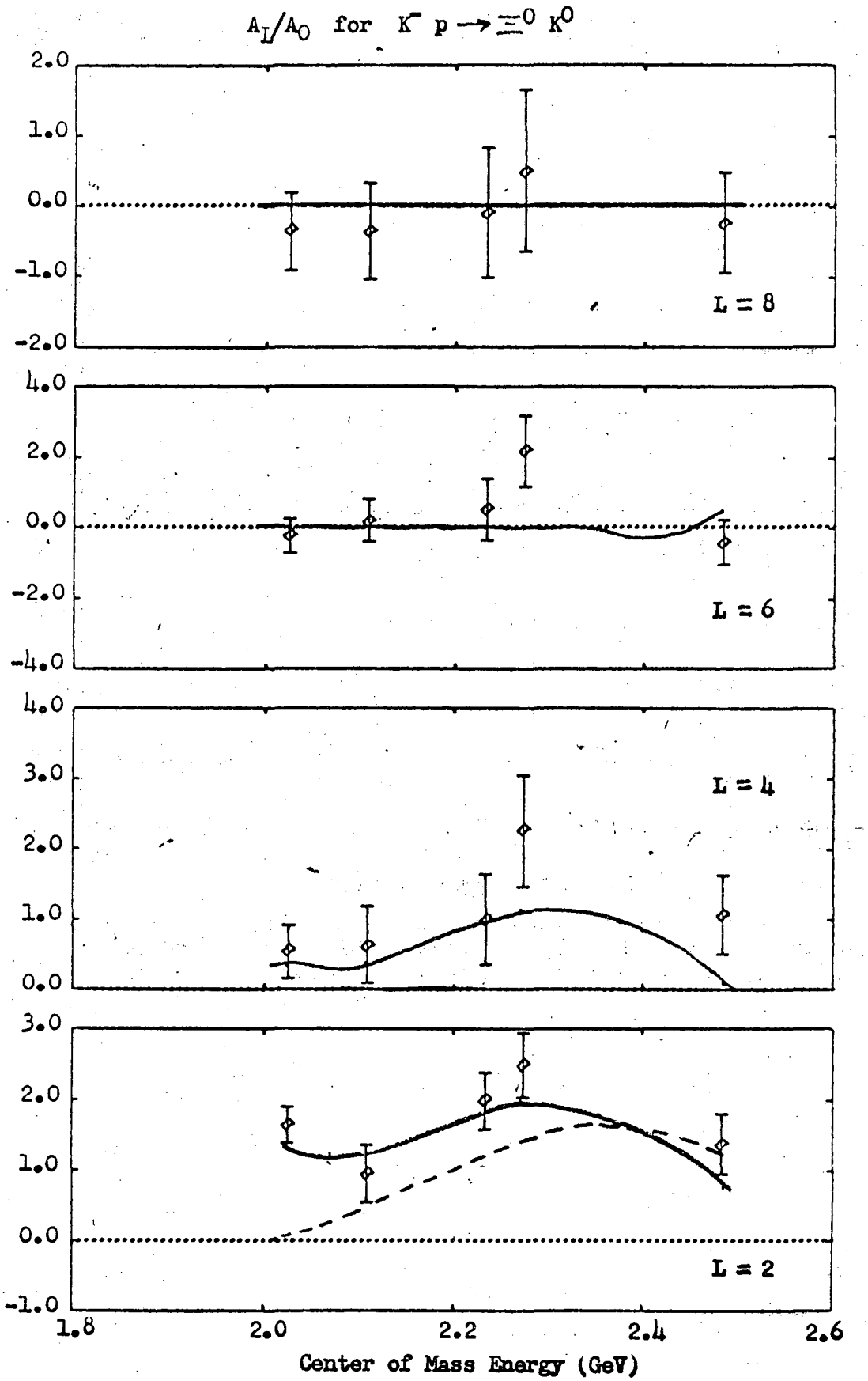

Figure 14. Legendre expansion coefficients. The solid curve corresponds to the $\chi^2 = 372$ solution discussed in section V. The dashed curves corresponds to the same fit when the amounts of all the resonances are set = 0.

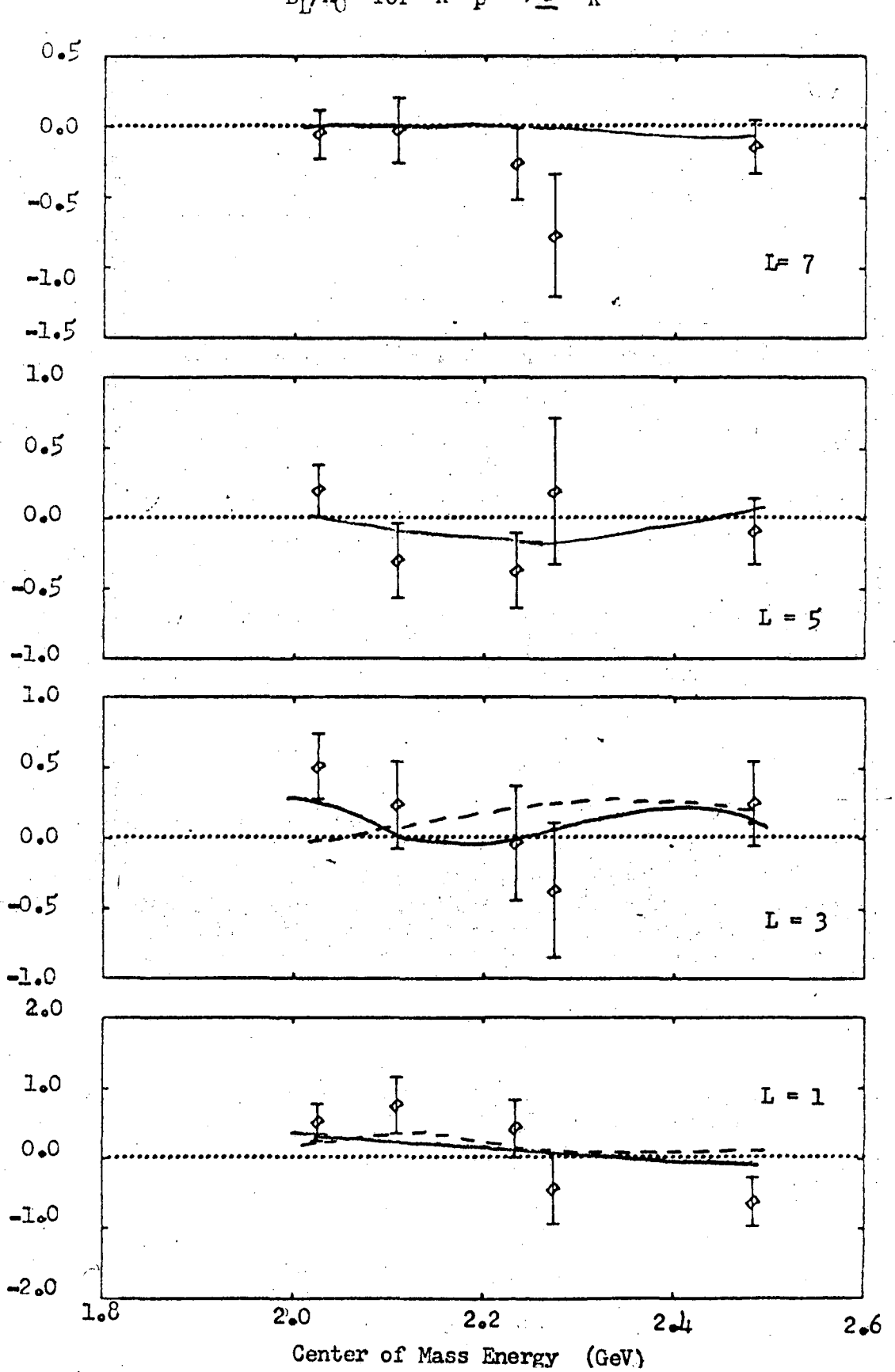

Figure 15. Legendre expansion coefficients. The solid curve corresponds to the $\chi^2 = 372$ solution discussed in section V. The dashed curves corresponds to the same fit when the amounts of all the resonances are set = 0.

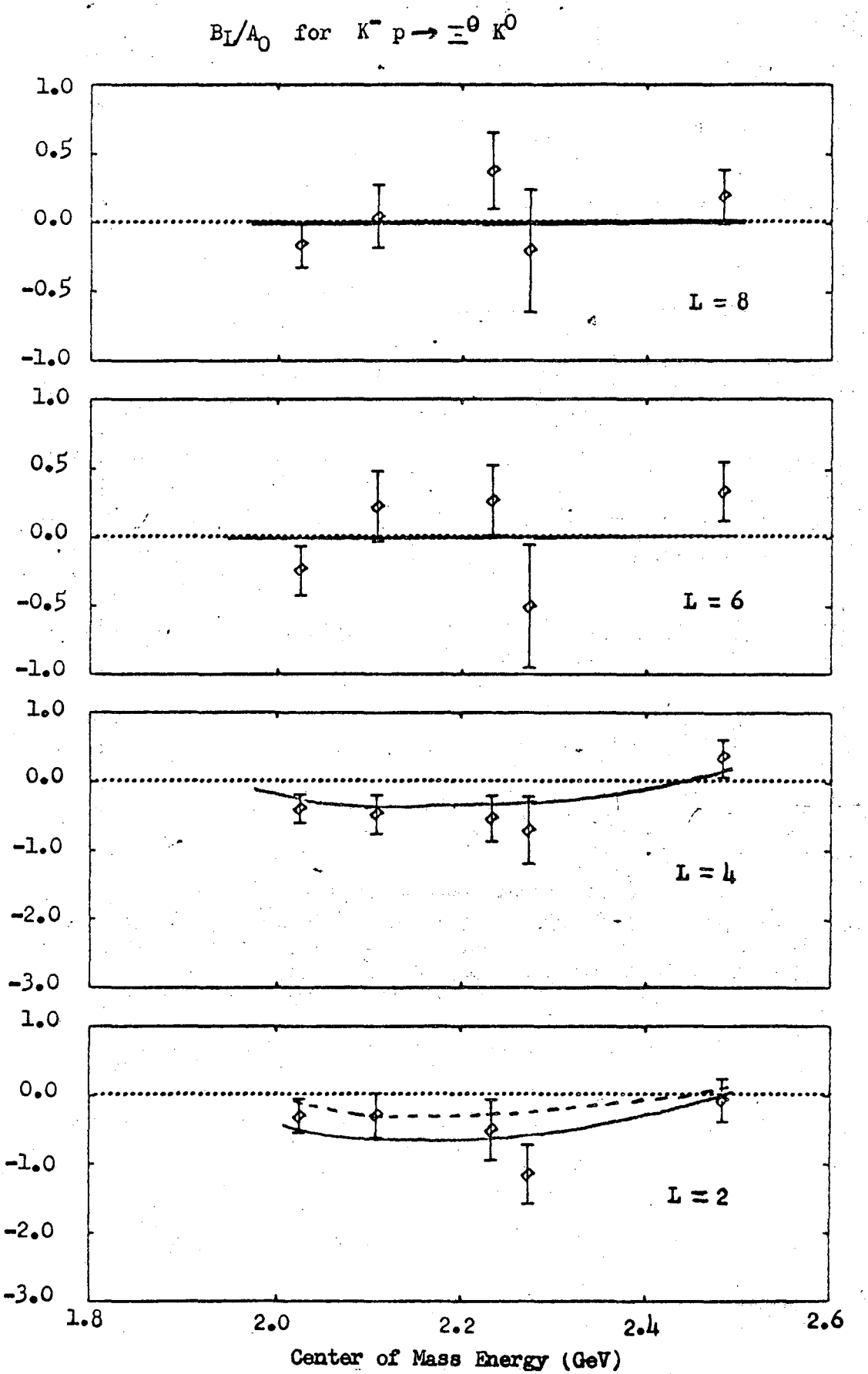

Figure 16. Legendre expansion coefficients. The solid curve corresponds to the $\chi^2 = 372$ solution discussed in section V. The dashed curves corresponds to the same fit when the amounts of all the resonances are set = 0.

2.0 GeV/c, and as previously noted, A_8 appears to be present at 2.64 GeV/c. In reactions (2) and (3) the statistics are poor, but A_5 is necessary for a good fit to the angular distributions in reaction (2), and in reaction (3) coefficients up to $\ell = 3$ are necessary.

B. Qualitative Interpretation

Figure 17 shows the baryon exchange diagrams for our three reactions. (Meson exchange would involve a strangeness 2 meson; we shall neglect this possibility.) We have indicated the quantum numbers of the exchanged particle by labeling it either a Λ or a $\Sigma^{\pm}$, although excited states of these particles could also be exchanged.

The data are most simply interpreted as being dominated by the exchange of an isotopic spin 0 baryon, with smaller (but important) contributions from I=1 exchange and resonances. The large backward peak could be generated from a u-channel pole, and its sharpening with energy could be partially due to its functional dependence on $u = (p_2-q_1)^2$. Since I=0 baryon exchange is forbidden in reaction 2, the amplitude for Ξ^0K^0 would consist of the smaller I=1 exchange and resonances--hence the smaller cross section. The rapid variation with energy in the differential cross section of reaction 2 would be accounted for by the relatively large contribution of the resonances. Likewise the high order Legendre expansion coefficients needed above 2.1 GeV/c would be due to the presence of one or more $J \gtrsim \frac{9}{2}$ resonances present at the higher energies.

C. Duality

The concept of "duality has recently received a good deal of attention.[12] In its strongest form the duality principle says that

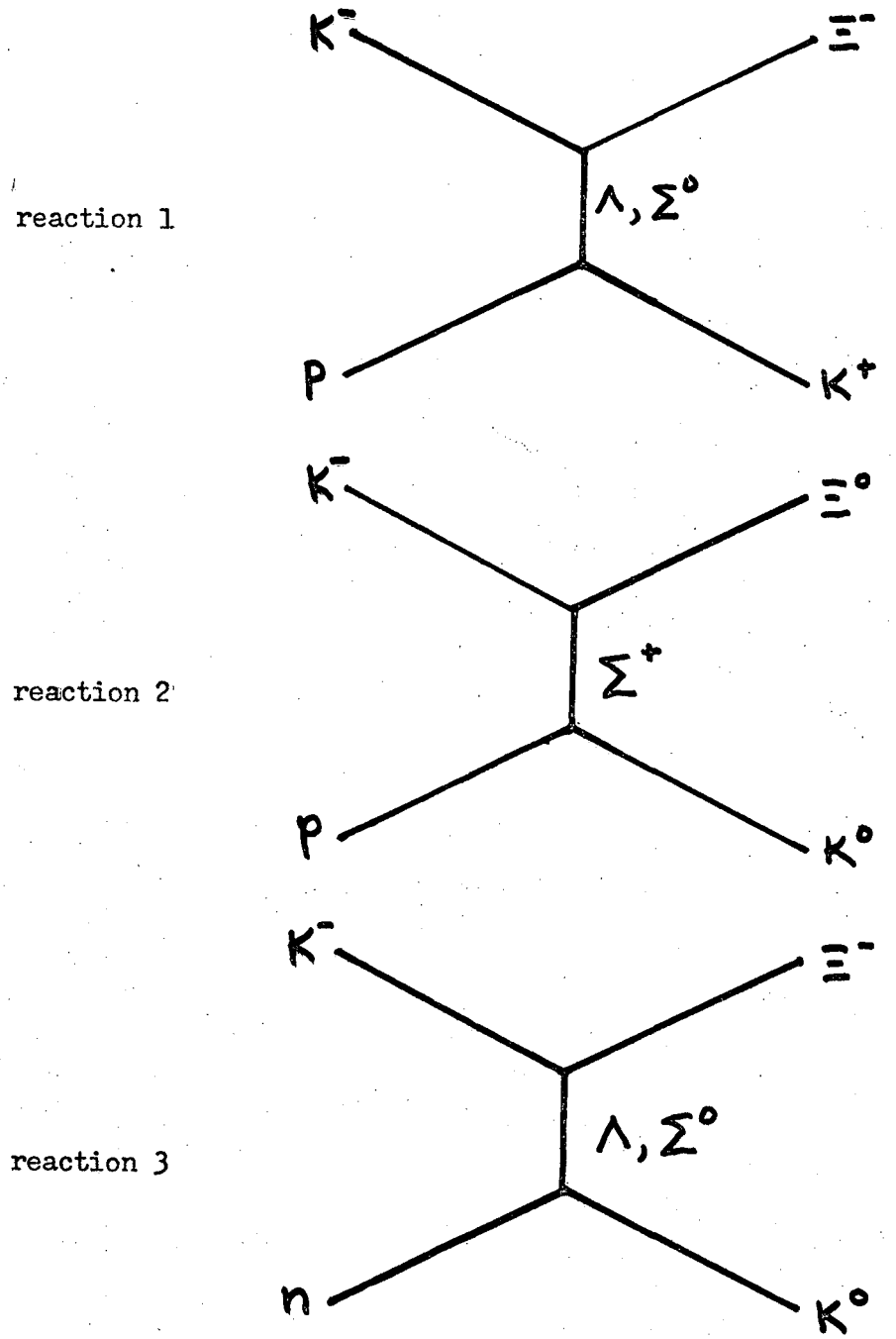

Fig. 17. Baryon Exchange Diagrams

the amplitudes for particle exchange and for resonant production are one and the same, and that if you add together particle exchange amplitudes and resonance represented by Breit-Wigner functions, you are engaged in "double counting". Since the previous qualitative discussion and the detailed fit in the next section seem to ignore this principle, some discussion is appropriate here.

The established resonances in the region we are studying are all in the higher partial waves, $J > \frac{3}{2}$. On the other hand, baryon exchange forces have a limited range, typically that of an inverse baryon mass. At our highest beam momentum (2.7 GeV/c) the incident center of mass momentum is $p_{cm} \approx 1$ GeV/c. Semi-classically we would expect the baryon exchange force to contribute only to the lower partial waves, up to

$$\ell \approx P_{cm}\, r_{max} \approx 1 \cdot \frac{1}{M_B} \lesssim 1$$

i.e., P wave. In other theories, such as a Regge exchange theory, the cut-off is not as clear since there are unknown residue factors. However, since the prominent "baryon-exchange" feature of our data, the backward peak, is well fit by the first three Legendre expansion coefficients, we shall assume that the part of the baryon exchange amplitude that produces this peak is confined to the lower partial waves, $D_{3/2}$ and lower.

Therefore, in our particular situation, duality poses no problem. We have one amplitude, whose lower partial waves behave like "baryon exchange" partial waves, and whose high partial waves behave like resonances. If it happens that the baryon exchange partial waves move

in counter-clockwise circles in the Argand plot with increasing energy, then the duality principle says we can also interpret these partial waves as resonant.[12]

V. MODEL

A. Baryon Exchange Amplitude

Partial wave analysis is particularly well suited to the study of resonances, since a resonance has definite spin and parity and therefore contributes to only one partial wave. Non-resonant partial waves are usually considered "background" and are often parameterized by simple polynomials. In our three reactions, however, the background seems to be confined to the lower partial waves, and it has properties (see Section IV) that indicate it is due to baryon exchange. We can make use of this knowledge to develop a parameterization for our "background" which is particularly suitable for our reactions.

Suppose our reactions were dominated by a single amplitude A represented by the baryon exchange diagram below:

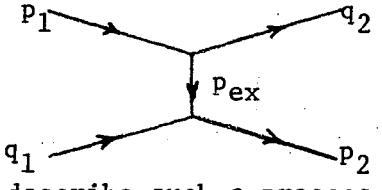

Natural variables to describe such a process are $s = (p_1 + q_1) = W^2$, and $u = p_{ex}^2 = (p_1 - q_2)^2$. (u is the square of the 4-momentum of the exchanged baryon.) Let us assume the amplitude A factorizes:

$$A(s,u) = S(s)\ U(u)$$

We believe that this is a reasonable assumption to make for a baryon exchange amplitude. The simple Born-Approximation baryon exchange model has this feature for spin-1/2 exchange, even if several baryons are exchanged.[5] Aside from a factor of $s^{\alpha(u)}$, so do simple Regge-exchange models.[13] A simple meson exchange amplitude does not have this feature (it factorizes into a function of s times a function of $t = (p_1-p_2)^2$)

and neither does a resonant amplitude (which factorizes into a function of s times a function of cosθ).

The factorization assumption generates powerful constraints on the energy dependence of the partial waves. To see how this comes about, let us ignore the complications of spin for the moment, and write the partial wave expansion of A(s,u),

$$A(s,u) = \sum_{L=0}^{LMAX} T_L(s)\ P_L(x)$$

where x = cos θ = known function of s and u.*

According to our factorization assumption,

$$U(u) = A(s,u)/S(s) = \sum T_L\ (s)\ P_L(x)/S(s)$$

U(u) is independent of the energy $W = \sqrt{s}$. Evaluating U(u) at two energies specified by s_1 and s_2,

$$\frac{1}{S(s_1)} \sum T_L\ (s_1)\ P_L\ (x(s_1, u)) = \frac{1}{S(s_2)} \sum T_L\ (s_2)\ P_L\ (x(s_2, u))$$

By using the orthogonality of the Legendre polynomials, we can solve for $T_L(s_1)$:

$$T_{L'}(s_1) = \frac{S(s_1)}{S(s_2)} \sum_{L=0}^{LMAX} R_{LL'}(s_1, s_2)\ T_L(s_2)$$

where

$$R_{LL'} = (L + \tfrac{1}{2}) \int_{-1}^{+1} P_L(x(s_1, u))\ P_L(x(s_2, u))\ dx$$

---

*x(s,u) is given explicity by $x = (-u + M_1^2 - m_2^2 - 2E_1E_2)/2p_1q_1$

where $E_1 = (S + M_1^2 + m_1^2)/2W$ $\quad p_1^2 = [S - (M_1 + m_1)^2] \cdot [S - (M_1 - m_1)^2]$

$E_2 = (S + m_2^2 - M_2^2)/2W$ $\quad p_2^2 = [S - (m_2 + M_2)^2] \cdot [S - (m_2 - M_2)^2]$

is a known function of s_1, s_2, and the particle masses.

The important feature is that aside from an overall normalization that is indendent of L, the partial waves at any energy may be calculated from the partial waves at any other energy, by multiplication by a known matrix. In other words, given a set of partial waves at energy W, the factorization assumption completely determines their relative energy dependences.

If we include the complications of spin we can still deduce a matrix relationship, but the derivation is complicated, and at least one arbitrary parameter must be included.[14] For the details, see the Appendix.

The matrix nature of the relationship is significant. It is a consequence of calling u rather than cosθ the important variable. Had we parameterized the individual partial waves with polynomials, for example, the low energy S wave would be related only to S waves at other energies. In our formalism it is related to S, P, and D waves at other energies.

By using the R matrix to give the relative energy dependences of the lower partial waves, we can construct the total normalized amplitude $\hat{A}(s,u) \equiv A(s,u)/|A(s,u)|$ given a set of partial waves at any one energy. If our reaction were completely dominated by baryon exchange we could do an energy dependent fit to the shape parameters, A_L/A_0 and B_L/A_0, using the set of partial waves at any one energy as our variables. (The shape parameters depend on $\hat{A}(s,u)$ rather than on $A(s,u)$.)

In order to include resonances in the fit, and to add together I=0

and I=1 baryon exchanges, it is necessary to make some assumption about the functional form of S(s). We have found that any function of the following general form works well:

$$S(s)=g\cdot(\text{threshold term})^{a}\cdot(\text{high energy fall off})\cdot\exp\left(i(c+ds+es^{2})\right)$$

Here g is a constant. "Threshold term" is any term that vanishes at threshold, such as p_2, or $(s-s_{threshold})$. "High energy fall off" is a term that causes the amplitude to go to zero at high energy. Such a term is reasonable in view of a compilation by Morrison[15] which shows that single particle exchange amplitudes (except for Pomeron exchange) fall off like $(P_{lab})^{-b}$ where $b > 0$. A term such as Morrison's, or a Regge s^{-b}, or a simple e^{-bs} all work equally well in the fit. The final term in the expression for S(s), a quadratic phase term, was necessary. We did not get good fits leaving the phase of S(s) constant or linear in s. We also tried the following functional forms for S(s):

$$S(s) = A+Bs+Cs^{2}$$

$$S(s) = A+Bp_{2}+Cp_{2}^{2}$$

where A, B, and C are complex numbers, and

$$S(s) = (A+Bs+Cs^{2})\cdot\exp(i(D+Es+Fs^{2}))$$

$$S(s) = (A+Bp_{2}+Cp_{2}^{2})\cdot\exp(i(D+Ep_{2}+Fp_{2}^{2})$$

where A, B, C, D, E, and F are real constants. None of the above parameterizations gave good fits.

B. Resonant Partial Waves

The higher partial waves were parameterized as Breit-Wigner functions with the masses and widths of established resonances. Only

the partial widths into our channel were free parameters. The form used for the Breit-Wigner was:[16,17]

$$T = \frac{W_0(\Gamma_1\Gamma_2)^{1/2}}{(W_0^2-W^2) - iW_0\,\Gamma_{tot}}$$

$$\Gamma_2 = \text{partial width into } \Xi K = \Gamma_0 \left(\frac{W_0}{W}\right) \left(\frac{q}{q_0}\right)^{2\ell+1} \left(\frac{q_0^2 + M^2}{q^2 + M^2}\right)^{\ell}$$

Γ_1 (the partial width for the elastic channel) and Γ_{tot} were taken to be constants because our energies are well above the elastic channel threshold. W_0 is the mass of the resonance, and q_0 is the final state center-of-mass momentum at resonance. M is a mass characteristic of the inverse range of the interaction. The fit is insensitive to the choice of M; we used $M = 2m_\pi$. We did not find it necessary to include background contributions in any of the resonant partial waves. Resonances near threshold are sensitive to the parameterization of the energy dependence of the width, but just above threshold they are not. For example, when we set the partial widths equal to constants the amount of the $Y_0^*(1830)$ put in by our fitting program changed considerably, but the amount of the $Y_1^*(2030)$ was virtually unaltered.

The fit included the following resonances:[18]

Resonance	Width (MeV)	Assumed Partial Wave
$Y_0^*(1815)$	75	F5
(1830)	80	D5
(1864)	39	F7
(2100)	140	G7
(2350)	210	G9 or H9
$Y_1(1915)$	60	F5
(2030)	120	F7
(2455)	120	G9 (best fit)
(2250)	200	H9 (best fit)
(2595)	140	I11(best fit)

C. The Fitting Program

The program used to fit A_0, A_L/A_0 and B_L/A_0 for our three reactions contained approximately 35 free parameters. These parameters were:

1. S_1, P_1, P_3, D_3 partial waves for I=0 and I=1 exchanges at any one energy W_0. (The fit is independent of W_0.)[19] From these the relative amplitudes and phases of the lower partial waves at all energies could be calculated. (8 complex numbers, 16 parameters)
2. Parameterization of f_s for I=0 and I=1 exchange. (See Appendix and footnote 14.) (2 parameters)
3. Parameterization of S(s) for I=0 and I=1 exchange. There are 4 parameters for each exchange. (See page 42. The parameters g and c are included in 1 above. 8 parameters.)
4. Resonant partial widths. (6-10 parameters)
5. D_5 complex partial wave for I=0 exchange above 2.4 GeV/c. (See page 46. 2 parameters)

The program used the equations derived in the Appendix (on the basis of the factorization assumption for the two Lorentz invariant amplitudes) to calculate the partial waves and Legendre expansion coefficients, A_L and B_L, at each of our beam settings.[20] We formed the chi-squared function:

$$\chi^2 = \sum \left(\frac{A_0 - A_0^{ex}}{\delta A_0^{ex}}\right)^2 + \left(\frac{a_\ell - a_\ell^{ex}}{\delta a_\ell^{ex}}\right)^2 + \left(\frac{b_\ell - b_\ell^{ex}}{\delta b_\ell^{ex}}\right)^2$$

where $a_\ell = A_\ell/A_0$ and $b_\ell = B_\ell/A_0$ are the shape parameters, the superscript "ex" refers to the experimental data points, and the sum ran over all

of our beam settings, over ℓ=1 to 8, and over all three reactions when we had data for them. This χ^2 was minimized by numerical minimizing program[21] which employed a ravine following search routine. When a solution was found we checked that the high order Legendre coefficients L > 8, which were not explicitly included in the fit, were compatible with zero.

D. Results of the Fit

We first fit the data in the region $1.2 \lesssim P_{lab} \lesssim 2.1$ GeV/c, assuming that no resonances were present. (The data above 2.1 were not included because of the presence of high Legendre coefficients, L > 4, which could not be due to the lower partial waves.) The solution accounted qualitatively for some of the general features of the data, especially the rise in A_2, but it certainly did not fit the reaction in detail. When the resonances listed on page 43 were included, a good fit was obtained, with a χ^2 of 281 for 296 data points.[22]

We restarted the fitting program, with random values for the parameters, approximately 15 times. The next best solution found had a χ^2 of 303. This fit had features very similar to those of the best fit; the amount and behavior of all the partial waves, resonant and non-resonant, was similar.

The spins and parities of the known resonances which might contribute to our reactions above 2.1 GeV/c have not yet been determined. In order to include the high energy data in our fit it was necessary to try various combinations of spins and parities for these resonances. The best fit was obtained with the combinations listed on page 43. In

addition we noticed that at 2.64 GeV/c the I=0 baryon exchange partial waves S_1, P_1, P_3, and D_3 were of comparable magnitude. Guessing that our cut-off at D_3 was too low, we tried including a D_5 I=0 exchange partial wave above 2.4 GeV/c; the χ^2 was reduced by about 15. The final fit had a χ^2 of 371 for 365 data points (solid line in Figures 8 to 16).

A Saclay-Rutherford collaboration has recently published[23] data for reactions (1) and (2) in the region $1.26 \leq P_{1ab} \leq 1.84$ GeV/c. When we used their data in our fit, including all our data below 2.4 GeV/c, we obtained a χ^2 of 525 for 504 data points. The parameters of the fit were not significantly altered by the inclusion of the Saclay data. Fitting their data alone yields a χ^2 of 211 for 208 data points. Including the $J^P = 3/2^{\pm}$ or $5/2^{\pm}$ resonance suggested by the Saclay fit did not substantially improve our χ^2. The major differences between our fit and Saclay's lie in our treatment of the lower partial waves (Saclay treated them as complex linear functions of the beam momentum) and our inclusion of all relevant resonances. For example, the Saclay group did not include the $Y_1^*(2030)$ in their fit because of its low elasticity, the absence of significant A_7, and the lack of a bump in the total cross section. In our fit (see Discussion) the $Y_1^*(2030)$ plays a major role despite these features.

Argand diagrams for the lower partial waves are shown in Figure 18. The amplitudes shown have definite isotopic spin in the u-channel. The contributions of the resonances to the fit are shown in Table 7. The errors were estimated by varying the amount of each resonance individually; the values correspond to an increase of χ^2 by unity. Also shown

Partial Wave Amplitudes of Definite

u-channel Isotopic Spin

Argand diagrams for $\chi^2 = 372$ fit

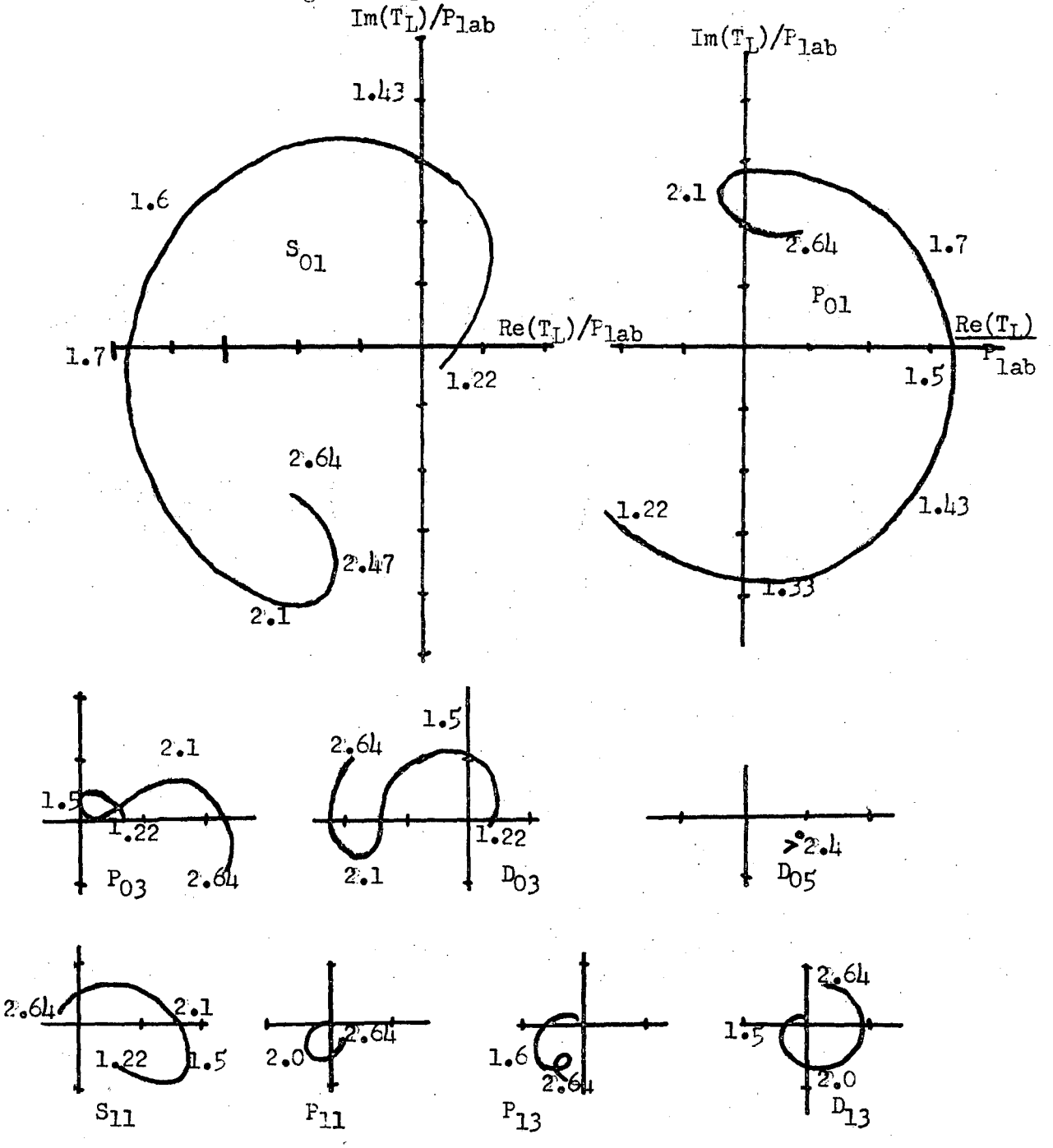

notation: $L_{2I_u,2J}$ one unit (⟷)=$(1\mu b)^{\frac{1}{2}}$

FIGURE 18

Table 7. Contributions of Resonances to $\chi^2 = 372$ Fit

Resonance	J^P	$-iT_I$ at resonance	χ^2 if $T_I = 0$	Contribution to A_0 for $\Xi^- K^+$
$Y_0^*(1815)$	$5/2^+$	$0.28 \pm .3 \times \sqrt{10^{-3}}$	373	0.23×10^{-3}
(1830)	$5/2^-$	$0.21 \pm .02$	515	0.13
(1864)	$7/2^+$	$-0.18 \pm .06$	381	0.11
(2100)	$7/2^-$	$0.10 \pm .05$	375	0.04
(2350)	$9/2^\pm$	$-0.15 \pm .12$	380	0.12
$Y_1^*(1915)$	$5/2^+$	$-0.26 \pm .07$	385	0.21
(2030)	$7/2^+$	$0.73 \pm .05$	560	2.10
(2250)	$9/2^+$	$0.20 \pm .05$	391	0.19
(2455)	$9/2^-$	$-0.12 \pm .05$	376	0.08
(2595)	$11/2^-$	$0.37 \pm .10$	388	0.08

is the effect on the χ^2 when the amount of that resonance is reduced to zero without permitting the other parameters to vary.

E. Discussion

The fit supports the qualitative interpretation given in section IV. As can be seen in the Argand plots, the reactions are dominated by I=0 baryon exchange. At low energies the baryon exchange amplitude is confined mostly to the S_1 and P_1 waves, but at the high energies P_3, D_3, and finally D_5 become important. The large S_1 and P_1 waves move counterclockwise in the complex plane as the energy increases. If we invoke the duality principle[12] to interpret these lower partial waves as resonances, we would need at least four new resonances: S_{01}, S_{11}, P_{01}, and P_{11} where the subscripts refer to 2I and 2J where I is the isotopic spin in the s-channel. Resonances of both s-channel isospins are necessary in order to keep the isospin 1 baryon exchange amplitude small through partial cancellation. (See page 7.)

The I=0 baryon exchange amplitude falls off at high energy as $(P_{lab})^{-1.5}$. This is consistent with the fall-off found by Morrison for other baryon-exchange processes.[15] (He found the exponent to vary between -1.5 and -2.0.) The I=1 baryon exchange amplitude falls off as $(P_{lab})^{-4.7}$; however, we do not consider our determination reliable because of the weakness of I=1 exchange in our reactions.

The baryon exchange amplitude contributes significantly to the polarization, as can be seen from the contribution it makes to the B_L's (dashed line in Figures 9-16). It is not surprising that the polarization does not come entirely from interferences with the resonances since, as we noted previously, the polarization distribution varies slowly with

energy. The fact that the polarization in the backward peak is small is related to the fact that the S_1 and P_1 I=0 exchange partial waves are almost relatively real. By this we mean that $Re(S_1/P_1) > Im(S_1/P_1)$ at all of our beam settings. This fact can also be seen in the Argand plots by noticing that the phases of the S_1 and P_1 partial waves differ by approximately 180°. It is interesting to note that for both Born-approximation and Regge exchange amplitudes, the partial waves are relatively real as long as only one particle is exchanged.

Although the lower partial waves dominate, resonance production in the higher partial waves is important at all energies. At our highest energy we are able to obtain a good fit by assigning the spins and parities listed on page 43 to the known resonances that might contribute in that region, but this high energy data is not good enough for us to be able to claim that we have determined those spins and parities. We have not tried all combinations which might give a good fit.

Only two resonances are essential to the fit: the $Y_0^*(1830)$ and the $Y_1^*(2030)$. The amounts of these resonances put in by the fit are relatively small, and their effect is primarily on the lower Legendre coefficients through interferences with the lower partial waves. For example, there is not enough $Y_1^*(2030)$ to generate a significant A_6, although this resonance contributes substantially to the shape of A_3 through its interference with the S_1 baryon exchange partial wave.

The inclusion of the $Y_0^*(1815)$ and the $Y_0^*(2100)$ have little effect on the fit. In an earlier paper[3] we interpreted the peak in A_0 near 1.7 GeV/c in reaction (1) and (2) as evidence for the $Y_0^*(2100)$ in those

reactions. The present fit does not completely account for the peaks in A_0, however, it is possible that the peaks are just statistical fluctuations.* In the region of the $Y_0^*(2100)$, if we include the Saclay total cross section data, our fits are about 2 standard deviations low in reaction (1) and about 2 standard deviations low in reaction (2). The Saclay-Rutherford collaboration[23] likewise concluded that the $Y_0^*(2100)$ does not make an important contribution to ΞK.

We tried to use our partial wave analysis to make an experimental determination of the parity of the Ξ. When we assume that the parity is negative (so that the $Y_1^*(2030)$ contributes to the F_{17} rather than to the G_{17} partial wave) we are again able to obtain a good fit to the low energy data. The fit yields a χ^2 of 284 for 296 data points, compared to a χ^2 of 281 assuming positive Ξ parity. We conclude that we are unable to determine the Ξ parity from our fitting procedure. Because of the indications of SU_3 that the Ξ parity is positive, we shall not discuss the negative parity solutions any further.

---

*We tried forcing the fit to include substantial $Y_0^*(2100)$. When we did this we got a better fit to A_0 but a much worse fit to A_3. The fit had a χ^2 of 460 for 365 data points.

VI. CONCLUSIONS

The reaction $K^- N \to \Xi K$ can be understood in terms of the exchange of one or more isotopic spin 0 baryons with small but important contributions from I = 1 exchange and direct channel resonance production. The known resonances are sufficient; there is no evidence for new resonances. At low energies the baryon exchange amplitude is mostly in the S_1 and P_1 partial waves, and these waves are "almost" relatively real. The baryon exchange amplitude is responsible for most of the small polarization. The large S_1 and P_1 partial waves move in counter-clockwise circles in the complex plane, suggesting that they may have a "dual" interpretation as resonant partial waves.

Because the data does not have significant high order Legendre coefficients in the region of the $Y^*(1830)$ and $Y^*(2030)$, we do not claim to have determined the branching fractions of these resonances into $\bar{K}\,\Xi$. In our data below 2.4 GeV/c these resonaces are seen only in the lower coefficients through interferences with the baryon exchange amplitude. (Perhaps if we had come up with a better parameterization of the function S(s) the fit would not have included either of these resonances!) Above 2.4 GeV/c there is strong evidence for the contributions of $J \gtrsim 9/2$ resonances.

Our approach has been different than that of many phase-shift analyses: instead of speculating about new resonances we have concentrated on a careful treatment of our "background". We think such an approach can make important contributions to an understanding of exchange mechanisms.

ACKNOWLEDGMENTS

I am very grateful to Luis W. Alvarez and Philip M. Dauber. I would also like to thank Lawrence H. Smith, Robert G. Smits, and Michael A. Wahlig.

APPENDIX

We outline here the derivation of the R-matrix for the scattering of a spin 0 boson off a spin 1/2 baryon. As discussed in section III, there are two invariant amplitudes A and B. We assume that both of these amplitudes factorize:

$$A(s,u) = S_A(s)\ U_A(u)$$

$$B(s,u) = S_B(s)\ U_B(u)$$

Using these equations, and explicitly writing out the partial wave expansion in terms of S, P, and D waves:

$$U_A = A(s,u)/S_A(s) = [(-W^+ - 3xW^-)D_3 + (3xW^+ + W^-)P_3 - W^-P_1 + W^+S_1]/S_A$$

$$U_B = B(s,u)/S_B(s) = [(-E^+ + 3xE^-)D_3 + (3xE^+ - E^-)P_3 + E^-P_1 + E^+S_1]/S_B$$

is related to $x(s_2,u)$ by the following kinematic formula:

$$x(s_2,u) = a + b \cdot x(s_1,u)$$

where

$$a = \frac{e_1(s_1)E_2(s_1) - e_1(s_2)E_2(s_2)}{q_1(s_2)\ p_2(s_2)}$$

$$b = \frac{q_1(s_1)\ p_2(s_1)}{q_1(s_2)\ p_2(s_2)}$$

The notation used is the same as that in section III. Evaluating U_A and U_B at s_1 and s_2, and then using the fact that they are independent of energy, we get:

$$\frac{1}{S_A(1)}\ [(-W_1^+ - 3xW_1^-)D_3(1) + (3xW_1^+ + W_1^-)P_3(1) - W_1^-P_1(1) + W_1^+S_1(1)]$$

$$= \frac{1}{S_A(2)}\ [(-W_2^+ - 3aW_2^- - 3bW_2^-x)D_3(2) + 3bW_2^+x + 3aW_2^+ + W_2^-)P_3(2) - W_2^-P_1(2) + W_2^+S_1(2)]$$

and:

$$\frac{1}{S_B(1)}\ [(-E_1^+ + 3xE_1^-)D_3(1) + (3xE_1^+ - E^-)P_3(1) + E_1^- P_1(1) + W_2^+ S_1(1)]$$

$$= \frac{1}{S_B(2)}\ [(-E_2^+ + 3aE_2^- + 3bE_2^- x)D_3(2) + (3bE_2^+ x + 3aE_2^+ - E_2^-)P_3(2) + E_2^- P_1(2) + E_1^+ S_1(2)]$$

The rest is simple, but messy, algebra. We have two equations, each linear in x. By equating the coefficients of x we generate four equations relating the four partial waves at one energy to the four partial waves at the second energy. We define the R-matrix by

$$\begin{pmatrix} S_1 \\ P_1 \\ P_3 \\ D_3 \end{pmatrix}_{s_2} = \frac{S_A(2)}{S_A(1)} \left(\underset{\sim}{R}(s_1, s_2)\right) \begin{pmatrix} S_1 \\ P_1 \\ P_3 \\ D_3 \end{pmatrix}_{s_1}$$

Its elements are listed in table A. Notice that R(s,s) is the identity matrix. The matrix R should satisfy the matrix relation:

$$R(s_1,s_2) = R(s_1,s_3)\ R(s_3,s_2)$$

We have not proven explicitly that our R matrix satisfies this relation, but we have checked numerically and found that it does.

TABLE A

The R-Matrix

Additonal symbols used: $f_s = S_B(2)\ S_A(1)/S_B(1)\ S_A(2)$

$$R_a = (-W_2^+ - 3aW_2^-)R_{43} + (3aW_2^+ + W_2^-)R_{33}$$

$$R_b = (-W_2^+ - 3aW_2^-)R_{44} + (3aW_2^+ + W_2^-)R_{34}$$

$$R_c = (-E_2^+ + 3aE_2^-)R_{43} + (3aE_2^+ - E_2^-)R_{33}$$

$$R_d = (-E_2^+ + 3aE_2^-)R_{44} + (3aE_2^+ - E_2^-)R_{34}$$

$$R_{44} = (-W_1^- E_2^+ - W_2^+ E_1^- f_s)/-b(W_2^- E_2^+ + W_2^+ E_2^-)$$

$$R_{43} = (W_1^+ E_2^+ - W_2^+ E_1^+ f_s)/-b(W_2^- E_2^+ + W_2^+ E_2^-)$$

$$R_{42} = 0$$

$$R_{41} = 0$$

$$R_{34} = (-W_1^- E_2^- + W_2^- E_1^- f_s)/\ b(W_2^+ E_2^- + W_2^- E_2^+)$$

$$R_{33} = (W_1^+ E_2^- + W_2^- E_1^+ f_s)/\ b(W_2^+ E_2^- + W_2^- E_2^+)$$

$$R_{32} = 0$$

$$R_{31} = 0$$

$$R_{24} = (-W_1^+ E_2^+ + W_2^+ E_1^+ f_s - E_2^+ R_b + W_2^+ R_d)/-(W_2^- E_2^+ + E_2^- W_2^+)$$

$$R_{23} = (W_1^- E_2^+ + W_2^+ E_1^- f_s - E_2^+ R_a + W_2^+ R_c)/-(W_2^- E_2^+ + E_2^- W_2^+)$$

$$R_{22} = (-W_1^- E_2^+ - W_2^+ E_1^- f_s)/-(W_2^- E_2^+ + E_2^- W_2^+)$$

$$R_{21} = (W_1^+ E_2^+ - W_2^+ E_1^- f_s)/-(W_2^- E_2^+ + E_2^- W_2^+)$$

$$R_{14} = (-W_1^+ E_2^- - W_2^- E_1^+ f_s - E_2^- R_b - W_2^- R_d f_s)/(E_2^- W_2^+ + W_2^- E_2^+)$$

$$R_{13} = (W_1^- E_2^- - E_1^- W_2^- f_s - E_2^- R_a - W_2^- R_c f_s)/(E_2^- W_2^+ + W_2^- E_2^+)$$

$$R_{12} = (-W_1^- E_2^- + W_2^- E_1^- f_s)/(E_2^- W_2^+ + W_2^- E_2^+)$$

$$R_{11} = (W_1^+ E_2^- + W_2^- E_1^+ f_s)/(E_2^- W_2^+ + W_2^- E_2^+)$$

FOOTNOTES AND REFERENCES

1. J. P. Berge, P. Eberhard, J. R. Hubbard, D. W. Merrill, J. B. Shafer, F. T. Solmitz, and M. L. Stevenson, Phys. Rev. 147, 945 (1966).
2. T. G. Trippe and P. E. Schlein, Phys. Rev. 158, 1334 (1967).
3. P. M. Dauber, J. P. Berge, J. R. Hubbard, D. W. Merrill, and R. A Muller, Phys. Rev. 179, 1262 (1969).
4. G. M. Pjerrou, "The Properties of Ξ^- and Ξ^0 Hyperons", Ph.D. Thesis, University of California at Los Angeles, 1965 (unpublished).
5. M. R. Ebel and P. B. James, Phys. Rev. 153, 1964 (1967).
6. P. B. James, Phys. Rev. 158, 1617 (1967).
7. J. T. Donohue, Ph.D. Thesis, University of Illinois, 1966 (unpublished).
8. Recently forward peaking in the reaction $K^- p \to \Xi^{*-} K^+$ has been observed which might be accounted for by the exchange of an "exotic" (strangeness or charge = 2) meson. See, for example, P. M. Dauber, P. Hoch, R. J. Manning, D. M. Siegel, M. A. Abolins and G. A. Smith, Phys. Letters (to be published).
9. R. D. Trippe, Proceedings of the International School of Physics "Enrico Fermi", Course XXXIII (Varenna, Italy, 1966) p. 70.
10. T. Trippe and P. Schlein, Partial Wave Expansion Coefficients Up to I-wave, UCLA High Energy Group Note No. 22, October 1965. I would like to thank Dr. Thomas Trippe for permission to reproduce Table 1 from his Ph.D. thesis.
11. The (-) sign in front of the $\bar{K}^0$ is necessary. For a discussion of this sign see C. Zemach, Appendix II in Rev. Mod. Phys. 41, 109 (1969).
12. C. Schmid, Phys. Rev. Letters 20, 689 (1968), and H. Harari, Proceedings of the 14th International Conference on High Energy Physics (Vienna, 1968) p. 195.

13. The an example of Regge-pole analysis using baryon exchange, see V. Barger and D. Cline, Phys. Rev. 155, 1792 (1967).

14. We have parameterized $f_s = S_B(2)\ S_A(1)/S_B(1)\ S_A(2)$ as $f_s = (s_2/s_1)^p$.

15. Chan Hong Mo, Proc. Conf. on High Energy 2-Body Reactions, (Stony Brook, N.Y., 1966) p. 391.

16. J. D. Jackson, Nuovo Cimenta 34, 1644 (1964).

17. S. L. Glashow and A. H. Rosenfeld, Phys. Rev. Lett. 10, 192 (1963).

18. We used all the Y^* resonances in our energy range in the compilation by N. Barash-Schmidt, A. Barbaro-Galtieri, L. R. Price, A. H. Rosenfeld, P. Soding, and C. G. Wohl, Rev. Mod. Phys. 41, 109 (1969).

19. For the fit to be independent of W_0 the R matrix must satisfy the matrix equation $R(s_1,s_2) \cdot R(s_2,s_3) = R(s_1,s_3)$. We numerically checked our R matrix to see that it had this property. In addition we tried the fit using a different W_0 and got the same solution.

20. I would like to thank Dr. Thomas Trippe for his subroutine CALCAB which calculates the A_L's and B_L's given the T_L's.

21. Stephen E. Derenzo, Alvarez Group Programming Memo No. 189, 1969 (unpublished).

22. A χ^2 of 281 for 296 data points with 35 parameters has a "confidence level" of approximately 4%. However, the confidence level is a very sensitive function of χ^2 in this region. A change in the error estimate of ±5% would lead to confidence levels of 0.1% or 15%. Rather than state the nominal confidence level for each fit, which we feel would be misleading, we shall merely give the χ^2 and the number of data points. The number of parameters for each of the fits is approximately 35.

23. G. Burgun, J. Meyer, E. Pauli, B. Tallini, J. Vrana, A. De Bellefon, A. Merthon, K. L. Rangan, J. Beaney, S. M. Deen, C. M. Fisher, and J. R. Smith, Nuclear Physics B8, 447 (1968).

TECHNICAL INFORMATION DIVISION
LAWRENCE RADIATION LABORATORY
UNIVERSITY OF CALIFORNIA
BERKELEY, CALIFORNIA 94720